Green's Function for Forcing of a Thin Floating Plate

Colin Fox and Hyuck Chung

Abstract

The Green's function for harmonic downward forcing of an infinite thin floating plate is derived. The Green's function models the response of a uniform sheet of fast ice when locally loaded at rates at which the ice may be taken to be elastic. A closed-form expression is given for the potential throughout the water and detailed expressions are given for the vertical displacement of the ice sheet. The displacement is graphed for various typical thickness of the ice sheet and for a range of frequencies of forcing.

Contents

1 Introduction 2
2 The Green's Function 2
2.1 Mathematical formulation 2
2.2 Spatial Fourier Transform 3
2.3 Inverse Fourier Transform 4
2.4 Residues of $\eta(k)$ 6
2.5 Residues of $\phi(k,0)$ 6
2.6 Summary of finding Green's function 7
3 Surface displacement in special cases 8
3.1 Surface displacement at the point of forcing 9
3.2 Surface displacement in the near field 10
3.3 Displacement in the far field 12
3.4 Static forcing 12
3.5 Deep water case 13
4 Surface strain 16
4.1 Strain in the near field 16
4.2 Strain in the far field 17
5 Some results in graph form 19
5.1 Residues 19
5.2 Surface displacement 20
5.3 Surface strain 21
A Special functions 24
B Series expansion of $\eta(k)$ 24
B.1 Series expansion of fractional functions 24
B.2 Conditions for $\eta(k)$ 26
B.3 Expansion of $\eta(k)$ 28
C MatLab code 29
C.1 Root finding code 29
C.2 Code for displacement and strain 33

1 Introduction

The New Zealand Programme in Sea-Ice Studies has a long standing interest in the coupling of ocean waves to shore-fast ice, and the resulting fatigue that produces break-up and other phenomena of geophysical importance (Fox et. al.[1]). That coupling is completely determined once the propagation of waves (including evanescent waves) is characterized in the open sea and ice covered sea. Since the propagation of ocean waves is well understood, our interest turns to characterizing wave propagation in an ice cover. That process is simple to describe for an infinite homogeneous cover, but the effective large-scale properties of a typical inhomogeneous cover are not known.

As a first step towards theoretically determining the large-scale propagation characteristics of inhomogeneous sea ice, we derive the Green's function for local forcing of an infinite homogeneous ice cover. It is intended that this "free-space" fundamental solution will be used within a boundary-integral formulation to express the propagation through a composite ice cover consisting of locally homogeneous pieces of ice joined by cracks, pressure ridges, steps in thickness, and other inhomogeneities

The Green's function also serves to predict expected results of an upcoming field experiment in which the surface strain due to local harmonic forcing will be measured. A device, which we call the Thumper, is being constructed within the New Zealand Programme to generate local forcing so that effective properties may be measured directly.

2 The Green's Function

2.1 Mathematical formulation

We consider the vertical forcing of a large sheet of floating sea ice. The sea ice is modelled as a thin plate (so has negligible thickness) at the surface of water of fixed depth H, as depicted in figure 1. Note that the surface is the plane $z = 0$ while the sea bottom is the plane $z = -H$. The x- and y-axes are taken to be in the plane of the ice sheet. The forcing is via a time-varying pressure p_{s} with restoring force – due to buoyancy and hydrodynamic effects – denoted by p_{w}.

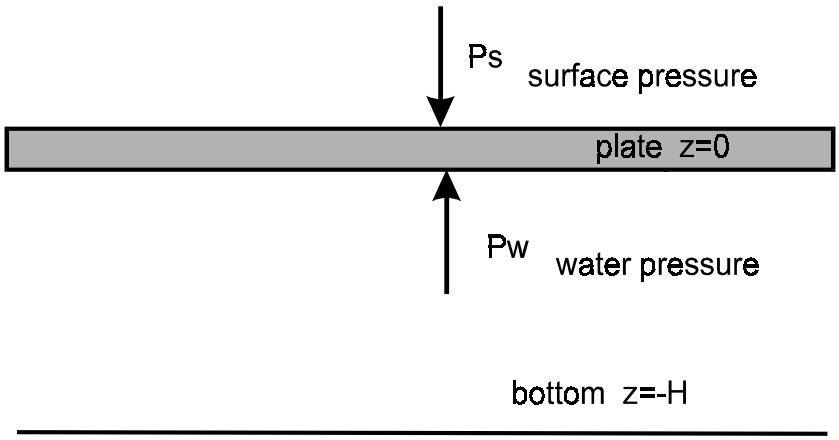

Figure 1:

The resulting mathematical model is given by the system of equations (Fox et. al.[1])

$$\left.\begin{array}{c} p_{\mathrm{i}} = L\nabla_{x,y}^4\eta + m\left(\eta_{tt} + g\right) + \beta\eta_t \\ p_{\mathrm{i}} = p_{\mathrm{w}} - p_{\mathrm{s}} \end{array}\right\} \quad \text{at } z = 0$$
$$\left.\begin{array}{c} \eta_t = \phi_z \\ \phi_t + \dfrac{p_{\mathrm{w}}}{\rho} + g\eta = 0 \end{array}\right\} \quad \text{at } z = 0 \tag{1}$$
$$\phi_z \to 0 \quad \text{as } z \to -H$$
$$\nabla_{x,y,z}^2\phi = 0 \text{ in the water}$$

where $\eta = \eta\left(x, y; t\right)$ is vertical displacement of ice from equilibrium, $\phi = \phi\left(x, y, z; t\right)$ is velocity potential in the water, ρ is density of water, $m = \rho_{\mathrm{i}}h$, ρ_{i} being density of ice and h is thickness of the ice sheet, and β is a damping coefficient which is a small positive number included to ensure that the model has a unique solution.

We will solve these equations for forcing p_{s} that is localized at the origin, $x = y = 0$, and that has harmonic time dependence, i.e.,

$$p_{\mathrm{s}} = \delta\left(x, y\right)\exp\left\{i\omega t\right\}. \tag{2}$$

The total force applied by this pressure is $1\exp\left\{i\omega t\right\}$ Newtons.

Since the physical properties, and the system of equations, is invariant under translations in the plane of the ice sheet, the response due to any localized harmonic forcing is found by shifting the response we derive. Note that all other possible (finite energy) forcing, with any given space and time dependence, is a linear combination of such forces and as the system is linear, the resulting motion is the same linear combination of responses. Since the system of equations is also invariant in time it follows that the functions η and ϕ have the same harmonic time dependence, in particular we note that $\phi\left(x, y, z; t\right) = \phi\left(x, y, z\right)\exp\left\{i\omega t\right\}$, and similarly for η. We will omit writing the $\exp\left\{i\omega t\right\}$ time dependence from now on, and take it to be implicit.

2.2 Spatial Fourier Transform

We will solve the system of equations 1 by taking the spatial Fourier transform of the localized forcing, in the plane of the ice sheet, solving the resulting equations in the spatial Fourier domain and then transform back to spatial variables. The spatial Fourier transform decomposes the delta-function spatial dependence into an integral over wave-like forcing functions

$$p_{\mathrm{s}}\left(\mathbf{k}\right) = \exp\left\{i\mathbf{k}\cdot\mathbf{x}\right\}$$

where $\mathbf{k} = \left(k_x, k_y\right)$ is the wave number that takes on all possible values in $\mathbb{R}^2$, and $\mathbf{x} = \left(x, y\right)$ is the spatial variable in the plane of the ice sheet. Define $k = \left\|\mathbf{k}\right\|$. Since the system is linear and invariant under shifts in the plane of the ice sheet, the functions ϕ and η will also have $\exp\left\{i\mathbf{k}\cdot\mathbf{x}\right\}$ dependence in the plane of the ice sheet. We will write the spatial transform of the functions ϕ and η as $\phi\left(k_x, k_y, z\right)$ and $\eta\left(k_x, k_y\right)$, respectively, and solve for those transform variables. That is, we use the same symbol for the transformed functions, the operation of the function is implicitly defined by the type of variables it takes as arguments.

Since the velocity potential ϕ satisfies Laplace's equation, the Fourier transform with respect to x and y satisfies the ordinary differential equation

$$\frac{\partial^2\phi}{\partial z^2}\left(k_x, k_y, z\right) - \left(k_x^2 + k_y^2\right)\phi\left(k_x, k_y, z\right) = 0$$

which can be solved to determine that $\phi(k_x, k_y, z) = A(k_x, k_y) e^{kz} + B(k_x, k_y) e^{-kz}$. The boundary condition on ϕ at $z = -H$ is $\phi_z(k_x, k_y, z = -H) = 0$ and hence $A(k_x, k_y) = Ce^{kH}$, and $B(k_x, k_y) = Ce^{-kH}$. Thus the depth-dependence of the potential due to the wave-like forcing is

$$\phi(k_x, k_y, z) = \phi(k_x, k_y, 0) \frac{\cosh k(z + H)}{\cosh kH}. \tag{3}$$

At the surface, $z = 0$, the vertical component of the velocity is

$$\phi_z(k_x, k_y, 0) = \phi(k_x, k_y, 0) k \tanh kH.$$

Using this relationship to substitute for ϕ_z, the system of equations 1 become, for the spatial Fourier transform of the functions ϕ and η,

$$\begin{array}{c} \left.\begin{array}{c} p_{\mathrm{i}} = Lk^4\eta - m\omega^2\eta + i\beta\omega\eta \\ p_{\mathrm{i}} = p_{\mathrm{w}} - 1 \end{array}\right\} \quad \text{at } z = 0 \\ \left.\begin{array}{c} i\omega\eta = \phi k \tanh kH \\ i\omega\phi + \dfrac{p_{\mathrm{w}}}{\rho} + g\eta = 0 \end{array}\right\} \quad \text{at } z = 0 \end{array} \tag{4}$$

Note that we have set $p_{\mathrm{s}} = 1$ as the coefficient of the $\exp\{i\mathbf{k} \cdot \mathbf{x}\}$ term in the forcing equals one. This system can be solved for the displacement of the ice sheet, η, the result being

$$\eta(k) = \frac{-1}{Lk^4 - m\omega^2 + \rho g + i\beta\omega - \dfrac{\rho\omega^2}{k \tanh kH}}. \tag{5}$$

Note that η is a function of the *magnitude* of the wave number only, which is not surprising as the geometry is circularly symmetric with no preferred direction of propagation. Note also that roots of the denominator are the solutions of the dispersion equation (Fox et. al.[1]). Hence we know that, for fixed $\omega \neq 0$ and for $\beta = 0$, there are two real roots corresponding to travelling waves, four complex roots corresponding to damped-travelling waves, and a countably infinite set of imaginary roots corresponding to evanescent modes. We will use the solution in the limit $\beta \searrow 0$ and so the roots are close to the ones described. Since the denominator is even, if k_0 is a root then so is $-k_0$.

The surface displacement in terms of spatial variables is the inverse 2-dimensional Fourier transform of $\eta(\mathbf{k})$.

We may also solve the system 4 for $\phi(k_x, k_y, 0)$; The result is

$$\phi(k_x, k_y, 0) = \frac{i\omega\eta}{k \tanh kH} = \frac{-i\omega}{k \tanh kH (Lk^4 - m\omega^2 + \rho g + i\beta\omega) - \rho\omega^2} \tag{6}$$

which is a function of k only and has the same poles as $\eta(k)$.

2.3 Inverse Fourier Transform

Here, we remind ourselves that the inverse Fourier transform of radially symmetric functions such as $\eta(k)$ is (Bracewell [2])

$$\eta(r) = \frac{1}{2\pi} \int_0^\infty \eta(k) k J_0(kr) \, dk$$

where $r = \|\mathbf{x}\|$ is the distance from the point of forcing. Note that the factor $1/2\pi$ is a result of the definition of the forward transform that we assumed.

For convenience we describe the poles in the absence of damping, i.e. when $\beta = 0$, but note that the positions of the poles will be slightly different when β is a small positive number. As the poles occur as positive and negative pairs, we select only those poles that lie in the upper-half plane when $\beta > 0$. Let k_{T} denote the real pole corresponding to travelling waves, k_{D} a complex pole corresponding to damped travelling waves choosing the pole with $\operatorname{Re} k_{\mathrm{D}} > 0$ and $\operatorname{Im} k_{\mathrm{D}} > 0$, and $\{ik_n\}_{n=1,2,\ldots}$ the imaginary poles giving evanescent modes. Note that $k_n \to \left(n - \frac{1}{2}\right)\pi/H$ as n increases. A second complex pole $-k_{\mathrm{D}}^*$ also lies in the upper half plane. Let $\hat{K} = \{k_{\mathrm{T}}, k_{\mathrm{D}}, -k_{\mathrm{D}}^*, ik_1, ik_2, ik_3, \cdots\}$ denote this set of poles. Note that the remaining poles are the negative of the poles in $\hat{K}$.

Since $\eta(k)$ is an even fractional function and bounded in the whole plane except in regions around the poles, η can be expressed as

$$\eta(k) = \sum_{\kappa \in \hat{K}} \frac{2\kappa R(\kappa)}{k^2 - \kappa^2}$$

where the sum is over the poles of $\eta(k)$ with positive imaginary part (in the case $\beta > 0$) and $R(\kappa)$ is the residue of η at κ. The validity of this expansion is derived in an appendix. The expansion allows us to use the identity (from Abramowitz and Stegun [4] formula 11.4.44 with $\nu = 0$ and $\mu = 0$)

$$\int_0^\infty \frac{k}{k^2 + z^2} J_0(ka)\, dk = K_0(za), \quad \operatorname{Re} z > 0, a > 0.$$

The identity (Abramowitz and Stegun [4] formula 9.6.4) $K_0(z) = \frac{\pi i}{2} H_0^{(1)}(iz)$ (holding for $\operatorname{Re} z \geq 0$) gives an alternative form.

These formulas applied with $z = -i\kappa$ and $a = r$ give

$$\int_0^\infty \frac{k}{k^2 - \kappa^2} J_0(kr)\, dk = K_0(-i\kappa r) = \frac{\pi i}{2} H_0^{(1)}(\kappa r)$$

for $\operatorname{Im} \kappa > 0$, $r > 0$. Thus,

$$\begin{aligned} \eta(r) &= \frac{1}{2\pi} \int_0^\infty \eta(k)\, k J_0(kr)\, dk \\ &= \frac{1}{2\pi} \int_0^\infty \sum_{\kappa \in \hat{K}} \frac{2\kappa R(\kappa)}{k^2 - \kappa^2} k J_0(kr)\, dk \\ &= \frac{1}{\pi} \sum_{\kappa \in \hat{K}} \kappa R(\kappa) K_0(-i\kappa r). \end{aligned} \tag{7}$$

Alternatively

$$\eta(r) = \frac{i}{2} \sum_{\kappa \in \hat{K}} \kappa R(\kappa) H_0^{(1)}(\kappa r). \tag{8}$$

Note that, as with plane-wave propagation, the real root (when $\beta = 0$) gives rise to a wave that propagates into the far field, the complex roots give damped travelling waves that decay exponentially away from the point of forcing, while the (close to) imaginary roots give modes that have no propagating component and decay rapidly away from the point of forcing.

2.4 Residues of $\eta(k)$

The residue $R(\kappa)$ at a pole κ of $\eta(k)$ can be found using the usual technique, i.e.,

$$\begin{aligned} R(k) &= \left.\frac{-1}{\left(Lk^4 - m\omega^2 + \rho g + i\beta\omega - \dfrac{\rho\omega^2}{k\tanh kH}\right)'}\right|_{k=\kappa} \\ &= -\left(4L\kappa^3 + \rho\omega^2\left(\frac{1}{\kappa^2\tanh(\kappa H)} + \frac{H}{\kappa}\left(\frac{1}{\tanh^2(\kappa H)} - 1\right)\right)\right)^{-1}. \end{aligned}$$

Since each pole κ satisfies the dispersion equation

$$L\kappa^5 + \left(\rho g - m\omega^2 + i\beta\omega\right)\kappa - \frac{\rho\omega^2}{\tanh\kappa H} = 0 \tag{9}$$

we may substitute $\tanh\kappa H = \rho\omega^2/\left(L\kappa^5 + a\kappa\right)$ where $a = \left(\rho g - m\omega^2 + i\beta\omega\right)$. So the residue may be given as the rational function of the pole

$$R(\kappa) = -\left(5L\kappa^3 + \frac{a}{\kappa} + \frac{H}{\kappa}\left(\frac{\left(L\kappa^5 + a\kappa\right)^2 - \left(\rho\omega^2\right)^2}{\rho\omega^2}\right)\right)^{-1}. \tag{10}$$

This form avoids calculation of the hyperbolic tangent which becomes small at the imaginary roots causing numerical roundoff problems.

We denote the residues for the poles in $\hat{K}$ by $R_{\mathrm{T}} = R(k_{\mathrm{T}})$, $R_{\mathrm{D}} = R(k_{\mathrm{D}})$, and $R_n = R(ik_n)$, $n \in \mathbb{N}$, respectively. Note that $R(-k_{\mathrm{D}}^*) \to -R_{\mathrm{D}}^*$ as the damping tends to zero.

For convenience we define

$$\mathcal{R}(\kappa) = R(\kappa)\,\kappa$$

for each $\kappa \in \hat{K}$. $\mathcal{R}(\kappa)$ is actually the residue of the function $\eta(k)\,k$ at its pole κ. Note that

$$\mathcal{R}(\kappa) = \frac{-\rho\omega^2\kappa^2}{\rho\omega^2\left(5L\kappa^4 + a\right) + H\left(\left(L\kappa^5 + a\kappa\right)^2 - \left(\rho\omega^2\right)^2\right)} \tag{11}$$

is an even function of κ and is real for κ real or pure imaginary. The values corresponding to the poles of interest are denoted $\mathcal{R}_{\mathrm{T}} = R_{\mathrm{T}}k_{\mathrm{T}}$, $\mathcal{R}_{\mathrm{D}} = R_{\mathrm{D}}k_{\mathrm{D}}$, and $\mathcal{R}_n = R_n ik_n$, $n \in \mathbb{N}$, respectively. The residue corresponding to the other damped-travelling pole $-k_{\mathrm{D}}^*$ is $\mathcal{R}_{\mathrm{D}}^*$.

Note that, as $|\kappa|$ increases, $|\mathcal{R}(\kappa)| \propto |\kappa|^{-8}$.

2 shows the residues (on a log-log plot) for the case $T = 10\mathrm{s}$, $H = 1000\mathrm{m}$, $h = 1\mathrm{m}$ and using $E = 6 \times 10^9$. The index is determined by the order the pole is listed in $\hat{K}$.

2.5 Residues of $\phi(k, 0)$

The residues of $k\phi(k, 0)$ are easily related to the residues $\mathcal{R}(\kappa)$ of $k\eta(k)$ via equation 6. The residue is

$$\mathcal{R}_\phi(\kappa) = \frac{i\omega\mathcal{R}(\kappa)}{k\tanh kH} = \frac{-i\omega\kappa\left(L\kappa^5 + a\kappa\right)}{\rho\omega^2\left(5L\kappa^4 + a\right) + H\left(\left(L\kappa^5 + a\kappa\right)^2 - \left(\rho\omega^2\right)^2\right)}$$

where we have used equation 11 and substituted the polynomial form of $\tanh kH$ as in the previous section. Note that these residues decrease as $|\kappa|^{-4}$as $|\kappa|$ increases.

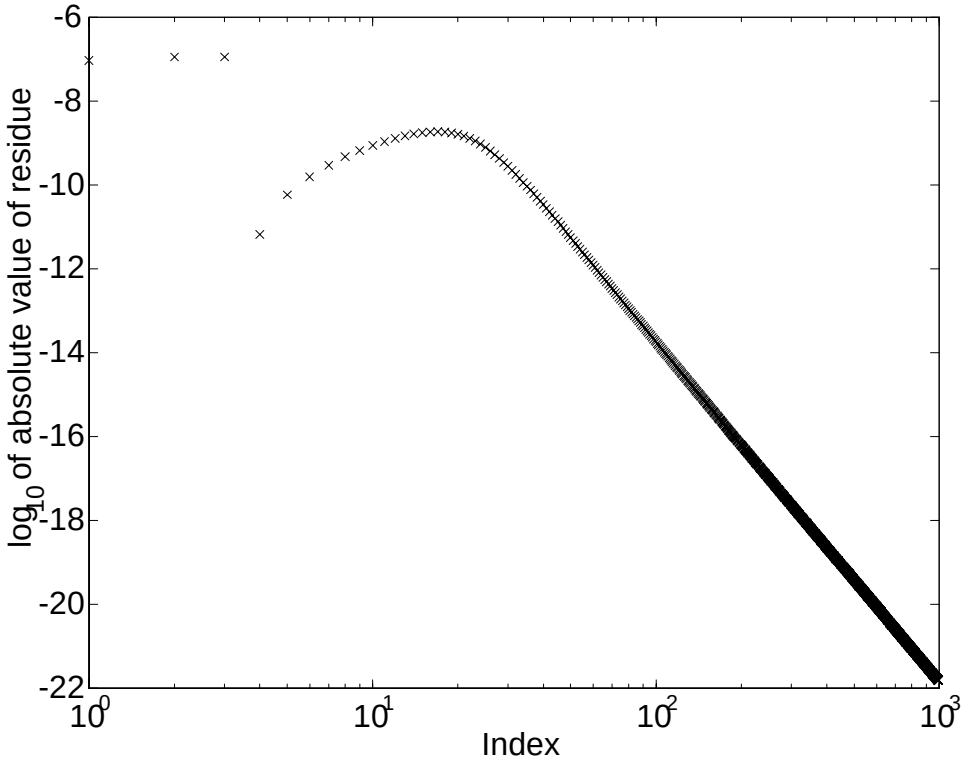

Figure 2: Magnitude of residues. Period of 10 seconds, water depth 1000 metres and ice thickness of 1 metre.

2.6 Summary of finding Green's function

The Green's function is found by first finding the roots in the upper-half plane $\hat{K} = \{k_{\mathrm{T}}, k_{\mathrm{D}}, -k_{\mathrm{D}}^*, ik_1, ik_2, ik_3, \cdots\}$ of the dispersion equation 10, calculating the residue for each root as in equation 11 and then computing the sum

$$\begin{aligned}
\eta(r) &= \frac{i}{2}\sum_{\kappa\in\hat{K}} \mathcal{R}(\kappa) H_0^{(1)}(\kappa r) \\
&= \frac{i}{2}\left(\mathcal{R}_{\mathrm{T}} H_0^{(1)}(k_{\mathrm{T}} r) + \mathcal{R}_{\mathrm{D}} H_0^{(1)}(k_{\mathrm{D}} r) + \mathcal{R}_{\mathrm{D}}^* H_0^{(1)}(-k_{\mathrm{D}}^* r) + \sum_{n=1}^{\infty} \mathcal{R}_n H_0^{(1)}(ik_n r)\right) \\
&= \frac{i}{2}\mathcal{R}_{\mathrm{T}} H_0^{(1)}(k_{\mathrm{T}} r) - \mathrm{Im}\left[\mathcal{R}_{\mathrm{D}} H_0^{(1)}(k_{\mathrm{D}} r)\right] + \frac{i}{2}\sum_{n=1}^{\infty} \mathcal{R}_n H_0^{(1)}(ik_n r). \qquad (12)
\end{aligned}$$

to find the resulting surface displacement. The step to the last line uses the identity $H_0^{(1)}(-z^*) = -\left(H_0^{(1)}(z)\right)^*$. Alternatively we may write

$$\begin{aligned}
\eta(r) &= \frac{1}{\pi}\sum_{\kappa\in\hat{K}} \mathcal{R}(\kappa) K_0(-i\kappa r) \qquad (13) \\
&= \frac{1}{\pi}\mathcal{R}_{\mathrm{T}} K_0(-ik_{\mathrm{T}} r) + \frac{2}{\pi}\mathrm{Re}\left[\mathcal{R}_{\mathrm{D}} K_0(-ik_{\mathrm{D}} r)\right] + \frac{1}{\pi}\sum_{n=1}^{\infty} \mathcal{R}_n K_0(k_n r) \qquad (14)
\end{aligned}$$

where we have used the identities $-i(-k_{\mathrm{D}}^*) = (-ik_{\mathrm{D}})^*$ and $K_0(z^*) = (K_0(z))^*$.

Here is a picture of surface displacement calculated using equation 12 with 1000 evanescent modes. Note that the graph is scaled for clarity. In this case many fewer would do.

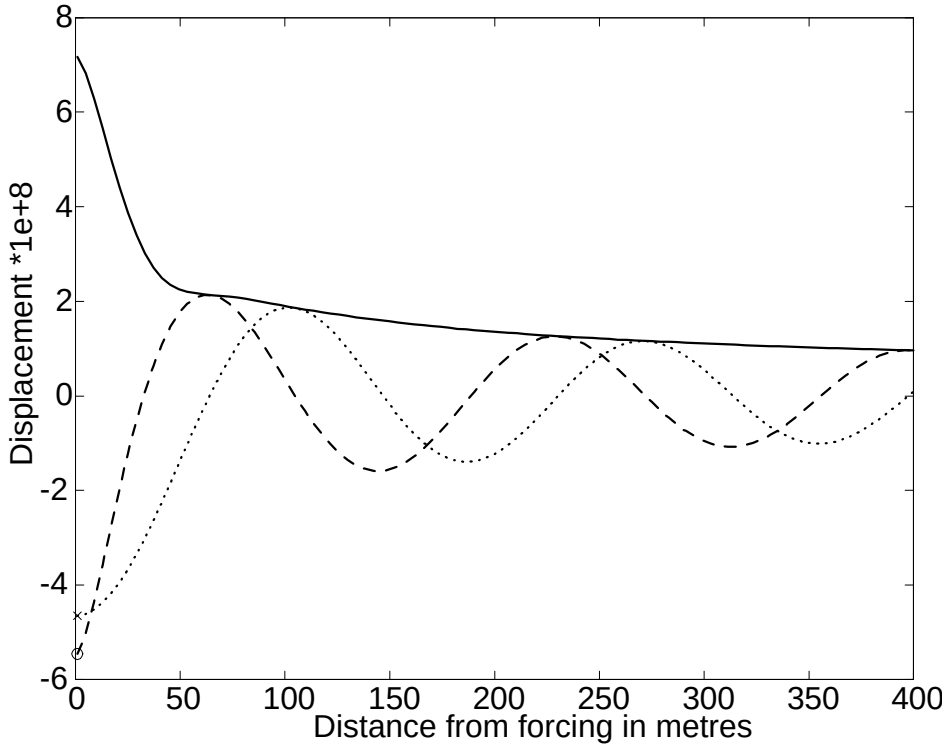

Figure 3: Surface displacement for the case Period of 10 seconds, water depth 1000 metres and ice thickness of 1 metre. Real part as dashed line, imaginary part as dotted line, magnitude as solid line.

The values at $r = 0$ marked, real value with an 'o' and imaginary value with an 'x'. Magnitude of forcing is 1Newton.

The potential throughout the water can be found by evaluating a similar inverse Fourier transform, with the residues changed. The resulting potential in cylindrical coordinates is

$$\phi(r,z) = \frac{i}{2} \sum_{\kappa \in \hat{K}} \mathcal{R}_\phi(\kappa) H_0^{(1)}(\kappa r) \frac{\cosh k(z+H)}{\cosh kH}. \tag{15}$$

Our main interest here is to determine surface displacement and strain for the purpose of designing experiments using strain gauges to detect the response due to the forcing. Consequently, we will not take this expansion for ϕ further.

3 Surface displacement in special cases

While the infinite sum in equation 12 gives the exact surface displacement at all $r \neq 0$, other forms are more convenient for some computational purposes. In the far field, i.e. when r is large, the number of terms that need to be summed is relatively few as the evanescent modes give no significant contribution. For very large r, the

asymptotic form of the Hankel function leads to a very simple expression for surface displacement. In the near field, i.e. when r is very small, the singularities in the imaginary part of the Hankel function leads to round-off error when using equation 12 directly; In that regime, using the form of the Bessel functions for small argument leads to a computationally stable expression.

3.1 Surface displacement at the point of forcing

The displacement function may be found for all $r > 0$ using either equation 12 or , 13. Strictly these expressions do not hold at the point of forcing $r = 0$ and, indeed, both expressions are the sum of terms that are singular at the origin, $r = 0$. However, since the plate equation is fourth order and Lapace's equation is second order, we would expect the solution to be smooth everywhere, including when $r = 0$. We study the infinite series more closely to find the displacement at $r = 0$.

The modified Bessel function $K_0(z)$ has the polynomial form

$$K_0(z) = -\log\left(\frac{z}{2}\right) I_0(z) + \sum_{l=0}^{\infty} \frac{(z/2)^{2l}}{(l!)^2} \psi(l+1),$$

where I_0 and ψ are the modified Bessel function and the Psi function, respectively (see appendix A for details). When $|z|$ is small, $K_0(z) \approx -\log z + c$ in which the constant $c = \log 2 - \gamma$. Hence, as $r \to 0$, the infinite series in 13 approaches

$$\begin{aligned}
\eta(r) &\to \frac{1}{\pi} \sum_{\kappa \in \hat{K}} \mathcal{R}(\kappa) \left(-\log(-i\kappa r) + c\right) \\
&= -\frac{1}{\pi}\left[\mathcal{R}_{\mathrm{T}} \log(-ik_{\mathrm{T}} r) + 2\,\mathrm{Re}\left[\mathcal{R}_{\mathrm{D}} \log(-ik_{\mathrm{D}} r)\right] + \sum_{n=1}^{\infty} \mathcal{R}_n \log(k_n r)\right] \\
&\quad + \frac{c}{\pi}\left[\mathcal{R}_{\mathrm{T}} + 2\,\mathrm{Re}(\mathcal{R}_{\mathrm{D}}) + \sum_{n=1}^{\infty} \mathcal{R}_n\right] \\
&= -\frac{1}{\pi}\left[\mathcal{R}_{\mathrm{T}} \log(-ik_{\mathrm{T}}) + 2\,\mathrm{Re}\left[\mathcal{R}_{\mathrm{D}} \log(-ik_{\mathrm{D}})\right] + \sum_{n=1}^{\infty} \mathcal{R}_n \log(k_n)\right] \\
&\quad + \frac{c - \log r}{\pi}\left[\mathcal{R}_{\mathrm{T}} + 2\,\mathrm{Re}(\mathcal{R}_{\mathrm{D}}) + \sum_{n=1}^{\infty} \mathcal{R}_n\right]. \qquad (16)
\end{aligned}$$

Consider a contour integration of the function $\eta(k)\,k$ along the path shown in Figure 4. The arc of radius R is chosen to avoid the poles, which is always possible as the number of poles in any bounded domain is finite (see appendix B).

Since $\eta(k)\,k$ is an odd function, the integral over the real axis is zero. Further, $\eta(k)\,k$ tends to zero faster than R^{-2} on the semi-arc as the radius, R, tends to infinity and so the integral over the semi-arc tends to zero as $R \to \infty$. Hence, the sum of residues at poles in the upper half plane is zero, i.e.,

$$\sum_{\kappa \in \hat{K}} \mathcal{R}(\kappa) = \mathcal{R}_{\mathrm{T}} + 2\,\mathrm{Re}(\mathcal{R}_{\mathrm{D}}) + \sum_{n=1}^{\infty} \mathcal{R}_n = 0.$$

Note that the residue at $k = -k_{\mathrm{D}}^*$ is $\mathcal{R}_{\mathrm{D}}^*$, so $\mathcal{R}_{\mathrm{D}} + \mathcal{R}_{\mathrm{D}}^* = 2\,\mathrm{Re}(\mathcal{R}_{\mathrm{D}})$.

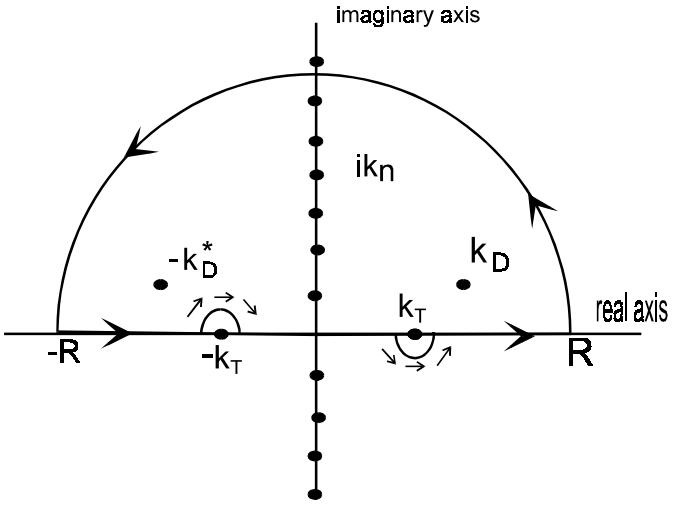

Figure 4: Contour used for integration with approximate pole positions shown.

We immediately see that the term multiplied by $(c - \log r)/\pi$ in equation 16 is zero. Thus at $r = 0$ the complex displacement takes the constant value

$$\begin{aligned}
\eta(0) &= -\frac{1}{\pi}\left[\mathcal{R}_{\mathrm{T}} \log(-ik_{\mathrm{T}}) + 2\,\mathrm{Re}\left[\mathcal{R}_{\mathrm{D}} \log(-ik_{\mathrm{D}})\right] + \sum_{n=1}^{\infty} \mathcal{R}_n \log(k_n)\right] \\
&= -\frac{1}{\pi}\left[\mathcal{R}_{\mathrm{T}}\left(\log(k_{\mathrm{T}}) - i\frac{\pi}{2}\right) + 2\,\mathrm{Re}\left[\mathcal{R}_{\mathrm{D}}\right]\log(k_{\mathrm{D}})\right. \\
&\quad \left. -2\,\mathrm{Im}\left[\mathcal{R}_{\mathrm{D}}\right]\left(\arg(k_{\mathrm{D}}) - \frac{\pi}{2}\right) + \sum_{n=1}^{\infty} \mathcal{R}_n \log(k_n)\right] \\
&= -\frac{1}{\pi}\left(\log\left\{(k_{\mathrm{T}})^{\mathcal{R}_{\mathrm{T}}}\,(k_{\mathrm{D}})^{2\,\mathrm{Re}\,\mathcal{R}_{\mathrm{D}}} \prod_{n=1}^{\infty} (k_n)^{\mathcal{R}_n}\right\} - 2\,\mathrm{Im}\left[\mathcal{R}_{\mathrm{D}}\right]\left(\arg(k_{\mathrm{D}}) - \frac{\pi}{2}\right)\right) \\
&\quad + i\frac{\mathcal{R}_{\mathrm{T}}}{2}.
\end{aligned}$$

Note that the values of wavenumbers with no damping have been used; All the wavenumbers and residuals are therefore real. Note that this formula gives the exact value of the displacement at the origin. Note that the more compact, equivalent, form

$$\eta(0) = -\frac{1}{\pi} \sum_{\kappa \in \hat{K}} \mathcal{R}(\kappa) \log(\kappa)$$

may also be used. Since $\mathcal{R}(\kappa)$ decreases as $k_n^{-8} \propto n^{-8}$ for the evanescent modes, relatively few terms are need to evaluate this sum.

A plot of $\eta(0)$ versus T is shown in figure 5 for various water depths.

Note that the smallest variation in the response is shown at small and large periods.

3.2 Surface displacement in the near field

Returning to the power series expansions of the Bessel function,

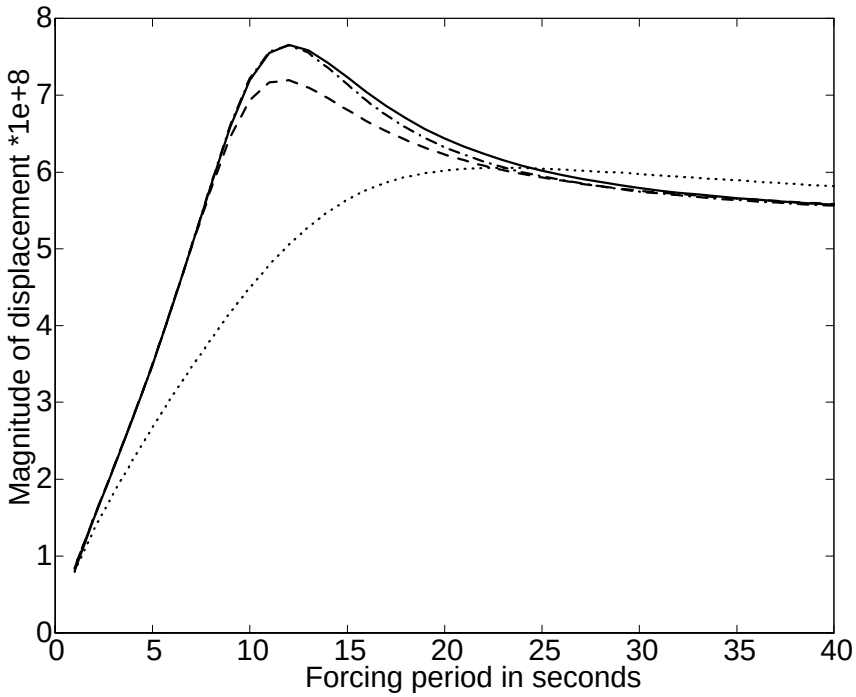

Figure 5: Plot of $\eta(0)$ versus T. Dotted line: Water depth 10m, Dashed line: 50m, Dashdot line:100m, Solid line: 1000m. Again the graph is scaled.

$$\begin{aligned}
\eta(r) &= \frac{1}{\pi}\sum_{\kappa\in\hat{K}}\mathcal{R}(\kappa)K_0(-i\kappa r) \\
&= \frac{1}{\pi}\sum_{\kappa\in\hat{K}}\mathcal{R}(\kappa)\left(\log\left(\frac{-i\kappa r}{2}\right)\sum_{l=0}^{\infty}\frac{(-i\kappa r/2)^{2l}}{(l!)^2}+\sum_{l=0}^{\infty}\frac{(-i\kappa r/2)^{2l}}{(l!)^2}\psi(l+1)\right) \\
&= \eta(0)+\frac{1}{\pi}\sum_{\kappa\in\hat{K}}\mathcal{R}(\kappa)\left(\sum_{l=1}^{\infty}\frac{(-i\kappa r/2)^{2l}}{(l!)^2}\left(\psi(k+1)-\log\left(\frac{-i\kappa r}{2}\right)\right)\right) \quad (17)
\end{aligned}$$

since the $l=0$ terms in the sums is dealt with in the previous section and gives the displacement at $r=0$.

Note that the terms with $l\geq 1$ have the r-dependence $(\log(\kappa r)+c)(\kappa r)^{2l}$ for some constant c. Since

$$\frac{d}{dr}(\log(\kappa r)+c)(\kappa r)^{2l}=\kappa^{2l}r^{2l-1}(1+2l(\log\kappa r+c))$$

these terms have zero derivative at $r=0$. Hence $\eta'(0)=0$ as expected. It follows that the displacement function obtained by the method above is regular everywhere.

Figure 6 shows the displacement calculated using the series in equation 17 directly.

As can be seen, the power series allows stable calculation for a range of r away from the point of forcing.

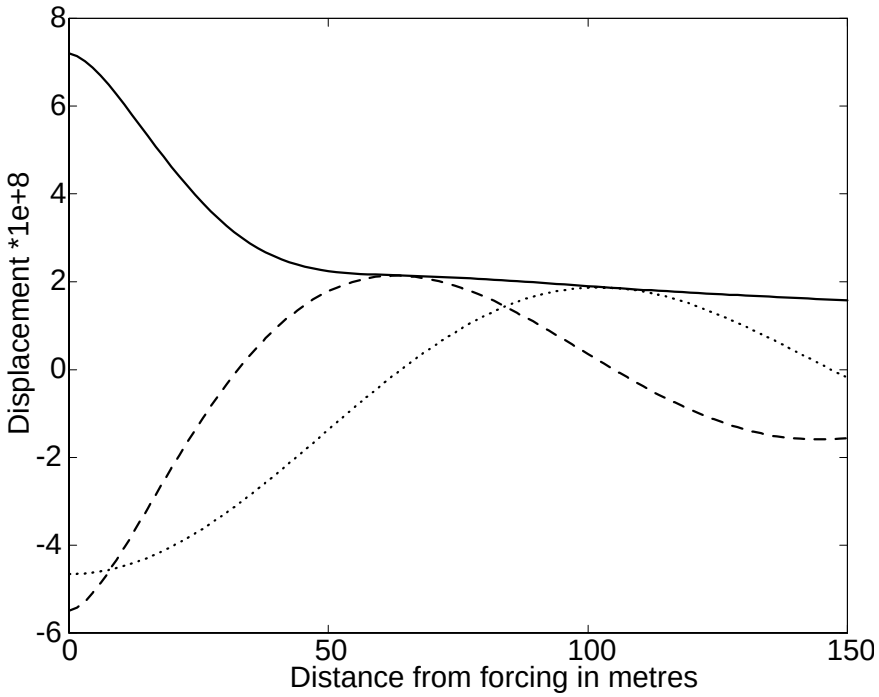

Figure 6: Dotted: imaginary part of the displacement function. Solid: real part. Dashed: absolute value. The constants used are, $H = 1000$ metres, $h = 1.0$ metres, period= 10 seconds. Number of evanescent modes added was 100.

3.3 Displacement in the far field

When $|z|$ is large then (Abramowitz and Stegun [4] formula 9.2.3)

$$H_0^{(1)}(z) \sim \sqrt{\frac{2}{\pi z}} \exp\left\{i\left(z - \pi/4\right)\right\}.$$

Thus, selecting just the term due to the travelling mode in equation **??** gives the complex displacement far from the point of forcing as

$$\begin{aligned} \eta(r) &\sim \frac{i\mathcal{R}_{\mathrm{T}}}{2}\sqrt{\frac{2}{\pi k_{\mathrm{T}} r}} \exp\left\{i\left(k_{\mathrm{T}} r - \pi/4\right)\right\} \\ &= \frac{\mathcal{R}_{\mathrm{T}}}{\sqrt{2\pi k_{\mathrm{T}}}} \frac{\exp\left\{i\left(k_{\mathrm{T}} r + \pi/4\right)\right\}}{\sqrt{r}} \end{aligned} \tag{18}$$

for large r.

3.4 Static forcing

The deflexion due to static point loading can easily be found using the method used to solve the dynamic case. That solution was previously given by Wymann[5], but we present an alternative derivation here as a check on our method and, in particular, the scaling.

Since the pressure is constant, we set $\omega = 0$ in equation 5 to give

$$\eta(k) = \frac{-1}{Lk^4 + \rho g}.$$

Now $\eta(k)$ has four complex poles, $k_1 = e^{i\pi/4}/l$, $k_2 = e^{i3\pi/4}/l$, $-k_1$, and $-k_2$ where $l = (L/\rho g)^{1/4}$ is the characteristic length of the ice sheet. The set of poles in the upper half plane is $\hat{K} = \{k_1, k_2\}$.

The residues of $k\eta(k)$ at a pole κ is

$$\mathcal{R}(\kappa) = \left.\frac{-\kappa}{(Lk^4 + g\rho)'}\right|_{k=\kappa} = \frac{-1}{4L\kappa^2}.$$

Hence $\mathcal{R}_1 = \mathcal{R}(k_1) = \dfrac{i}{4\rho g l^2}$ and $\mathcal{R}_2 = -\mathcal{R}_1$.

Using equation 13 we find

$$\eta(r) = \frac{1}{\pi}\frac{i}{4\rho g l^2}\left(K_0(-ik_1 r) - K_0(-ik_2 r)\right) = \frac{\mathrm{kei}(r/l)}{2\pi g\rho l^2}$$

where kei(x) is the Kelvin function (of zero order) and we have used the identity (Abramowitz and Stegun [4] formulas 9.9.2 and 9.6.32)

$$\mathrm{kei}(x) = \frac{K_0\left(e^{i\pi/4}x\right) - K_0\left(e^{-i\pi/4}x\right)}{2i}.$$

This expression is the same as given by Wymann and alternatively derived by Fox et. al.[6].

3.5 Deep water case

As the water depth becomes infinite, the poles of the evanescent modes become denser in proportion to the water depth and almost equally spaced with a spacing of $\frac{\pi}{H}$ on the imaginary axis. Then, we can see the formula 11 for the residue $\mathcal{R}(\kappa)$ as a function of a discrete variable $\kappa = in\pi/H$, $n = 1, 2, 3, ...$ We then have

$$\begin{aligned}
\mathcal{R}(\kappa) &= \frac{-b\kappa^2}{b\left(5L\kappa^4 + a\right) + H\left(\left(L\kappa^5 + a\kappa\right)^2 - b^2\right)} \\
&= \frac{1}{H}\frac{-b\kappa^2}{\frac{1}{H}\left(b\left(5L\kappa^4 + a\right)\right) + \left(\left(L\kappa^5 + a\kappa\right)^2 - b^2\right)} \\
&\to \frac{1}{H}\frac{-b\kappa^2}{\left(L\kappa^5 + a\kappa\right)^2 - b^2} = \frac{1}{H}Q(\kappa) \qquad (19)
\end{aligned}$$

as H becomes large. Hence, we have an approximation formula for integral, i.e.,

$$\begin{aligned}
\sum \mathcal{R}(\kappa) H_0^{(1)}(\kappa r) &\to \frac{1}{\pi}\sum_{n=1}^{\infty} Q\left(i\frac{n\pi}{H}\right) H_0^{(1)}\left(i\frac{n\pi}{H}r\right)\frac{\pi}{H} \\
&\to \frac{1}{\pi}\int_0^{\infty} Q(ik) H_0^{(1)}(ikr)\, dk \\
&= \begin{cases} \frac{1}{\pi}\int_0^{\infty} \frac{-bk^2}{\left(Lk^5 + ak\right)^2 + b^2} H_0^{(1)}(ikr)\, dk \text{ or} \\ \frac{2}{i\pi^2}\int_0^{\infty} \frac{-bk^2}{\left(Lk^5 + ak\right)^2 + b^2} K_0(kr)\, dk \end{cases} \qquad (20)
\end{aligned}$$

where $b = \rho\omega^2$. Note that the variable has been changed to real. Finally, we have a Green's function for a deep water case,

$$\begin{array}{c}\eta(r) = \frac{i}{2}\left(\mathcal{R}_{\mathrm{T}} H_0^{(1)}(k_{\mathrm{T}} r) + \mathcal{R}_{\mathrm{D}} H_0^{(1)}(k_{\mathrm{D}} r) + \mathcal{R}_{\mathrm{D}}^* H_0^{(1)}(-k_{\mathrm{D}}^* r)\right. \\ \left. + \frac{1}{\pi}\int_0^\infty \frac{-bk^2}{(Lk^5+ak)^2+b^2} H_0^{(1)}(ikr)\, dk\right).\end{array} \tag{21}$$

We notice that the integration 20[1] can be computed analytically by a series expansion of function $Q(ik)$. Let us remind an integral transform (Abramowitz and Stegun [4] formula 11.4.47),

$$\int_0^\infty \frac{k^{-1/2-\nu}}{(k^2+a^2)} K_0(kr)\, dk = \frac{\pi^2}{4a^{\nu+1}} \sec(\nu\pi)\left[\mathbb{H}_\nu(ar) - Y_\nu(ar)\right], \tag{22}$$

when $\mathrm{Re}\, r > 0, \nu < \frac{1}{2}, |\arg a| < \pi, \mathrm{Re}\, a > 0$. $\mathbb{H}_\nu$ is a Struve function (Abramowitz and Stegun [4] formula 12.1.3),

$$\mathbb{H}_\nu(z) = \sum_{m=0}^{\infty} (-1)^m \frac{(z/2)^{2m+\nu+1}}{\Gamma\left(m+\frac{3}{2}\right)\Gamma\left(\nu+m+\frac{3}{2}\right)}$$

Since, function $Q(ik)$ is even, by the same derivation previousl usedy in subsection 2.3, we have

$$Q(ik) = \sum_{n=1}^{5}\left(\frac{R_n}{k-a_n} - \frac{R_n}{k+a_n}\right) = \sum_{n=1}^{5}\frac{2a_n R_n}{k^2-a_n^2} \tag{23}$$

where $\{a_n\}$ are five poles of $Q(ik)$ with positive imaginary part and R_n is a residue at $k = a_n$. In order to use formula 22, we set $a = -ia$ and $\nu = 0$. We then have

$$\int_0^\infty \frac{1}{k^2-a^2} K_0(kr)\, dk = \frac{i\pi^2}{4a}\left[\mathbb{H}_0(-iar) - Y_0(-iar)\right], \quad \mathrm{Im}\, a > 0.$$

Hence, integration 20 becomes

$$\sum_{n=1}^{5}\int_0^\infty \frac{2a_n R_n}{k^2-a_n^2} K_0(kr)\, dk = \sum_{n=1}^{5}\frac{i\pi^2 R_n}{2}\left[\mathbb{H}_0(-ia_n r) - Y_0(-ia_n r)\right].$$

Hence, the formula 21 becomes

$$\begin{array}{c}\eta(r) = \frac{i}{2}\left(\mathcal{R}_{\mathrm{T}} H_0^{(1)}(k_{\mathrm{T}} r) + \mathcal{R}_{\mathrm{D}} H_0^{(1)}(k_{\mathrm{D}} r) + \mathcal{R}_{\mathrm{D}}^* H_0^{(1)}(-k_{\mathrm{D}}^* r)\right. \\ \left. \sum_{n=1}^{5} R_n\left[\mathbb{H}_0(-ia_n r) - Y_0(-ia_n r)\right]\right).\end{array} \tag{24}$$

We notice that function $Q(k)$ in equation 19 is a combination of the dispersion equation for a deep water case, i.e.,

$$\begin{aligned}\eta(k) &= \frac{-1}{Lk^4 + a - \frac{b}{k}}, \\ Q(k) &= \frac{k}{2}\left(\eta(k) - \eta(-k)\right),\end{aligned} \tag{25}$$

[1] Integration of this form is called K-transform or Meijer formula (Bateman [7])

$$g(y) = \int_0^\infty f(x)\sqrt{xy} K_\nu(xy)\, dx, f(x) = \int_0^\infty g(y)\sqrt{xy} I_\nu(xy)\, dy.$$

which can be obtained by following the same procedure in subsection 2.2 with a boundary condition at $z = -\infty$. It is apparent that the poles, a_n, and the residues, R_n, in formula 24 are related to k_{T} and k_{D} in equation 12. Figure 7 shows the positions of the poles of function 25 when the forcing period is ten seconds and the ice thickness is one metre.

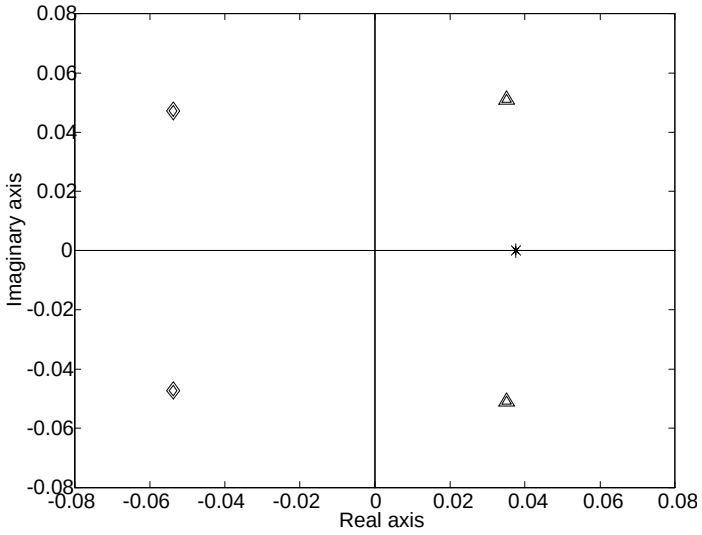

Figure 7: Poles of $\eta(k)$ for a deep water case. The forcing period is ten seconds and the ice thickness is one metre.

Let the poles shown above be $\{k_{\mathrm{T}}, k_{\mathrm{D}}, k_{\mathrm{D}}^*, k_{\mathrm{E}}, k_{\mathrm{E}}^*\}$ where '*' is k_{T}, 'triangle' is k_{D} and k_{D}^*, 'diamond' is k_{E} and k_{E}^*. We notice that

$$\{k_{\mathrm{T}}, k_{\mathrm{D}}, k_{\mathrm{D}}^*, -k_{\mathrm{E}}, -k_{\mathrm{E}}^*\} = \{-ia_n\}_{n=1,\ldots,5}.$$

We can see that $\{k_{\mathrm{T}}, k_{\mathrm{D}}, k_{\mathrm{D}}^*\}, \{-k_{\mathrm{E}}, -k_{\mathrm{E}}^*\}$ are poles of $\eta(k)$ and $\eta(-k)$ respectively. Hence, the residues, R_n, in equation 24 can be expressed with the residues, $\mathcal{R}(\kappa)$, $\kappa \in \{k_{\mathrm{T}}, k_{\mathrm{D}}, k_{\mathrm{D}}^*, -k_{\mathrm{E}}, -k_{\mathrm{E}}^*\}$.

$$\begin{aligned} R_n &= \lim_{k\to a_n} (k-a_n) Q(ik) = \lim_{k\to a_n} (k-a_n) \frac{ik}{2} (\eta(ik) - \eta(-ik)) \\ &= \lim_{k\to i\kappa} (k-i\kappa) \frac{ik}{2} (\eta(ik) - \eta(-ik)) = -\lim_{ik'\to i\kappa} (ik'-i\kappa) \frac{k'}{2} \left(\eta\left(-k'\right) - \eta\left(k'\right)\right). \end{aligned}$$

where $k' = -ik$. If κ is a pole of $\eta(k')$,

$$R_n = \frac{i}{2} \lim_{k'\to\kappa} \left(k'-\kappa\right) k'\eta\left(k'\right) = \frac{i}{2}\mathcal{R}(\kappa),$$

and if κ is a pole of $\eta(-k')$

$$R_n = -\frac{i}{2} \lim_{k'\to\kappa} \left(k'-\kappa\right) k'\eta\left(-k'\right).$$

Hence, for the poles $\{-k_{\mathrm{E}}, -k_{\mathrm{E}}^*\}$ we have

$$\begin{aligned} R_n &= -\frac{i}{2} \lim_{k'\to -k_{\mathrm{E}}} \left(k'+k_{\mathrm{E}}\right) k'\eta\left(-k'\right) = -\frac{i}{2} \lim_{k'\to k_{\mathrm{E}}} \left(k'-k_{\mathrm{E}}\right) k'\eta\left(k'\right) \\ &= -\frac{i}{2}\mathcal{R}(k_{\mathrm{E}}). \end{aligned}$$

Similarly, for $-k_{\mathrm{E}}^{*}$ we have $R_n = -\frac{i}{2}\mathcal{R}\left(k_{\mathrm{E}}\right)^{*}$. Hence, we can ultimately obtain a formula for the displacement function, $\eta\left(r\right)$, with the five poles of function 25,

$$\begin{aligned}\eta\left(r\right) &= \frac{i}{2}\mathcal{R}_{\mathrm{T}}\left[H_0^{(1)}\left(k_{\mathrm{T}}r\right)+\frac{i}{2}\left\{\mathbb{H}_0\left(k_{\mathrm{T}}r\right)-Y_0\left(k_{\mathrm{T}}r\right)\right\}\right]\\ &\quad -\mathrm{Im}\left[\mathcal{R}_{\mathrm{D}}H_0^{(1)}\left(k_{\mathrm{D}}r\right)\right]-\frac{1}{2}\mathrm{Re}\left[\mathcal{R}_{\mathrm{D}}\left\{\mathbb{H}_0\left(k_{\mathrm{D}}r\right)-Y_0\left(k_{\mathrm{D}}r\right)\right\}\right]\\ &\quad +\mathrm{Re}\left[\mathcal{R}_{\mathrm{E}}\left\{\mathbb{H}_0\left(-k_{\mathrm{E}}r\right)-Y_0\left(-k_{\mathrm{E}}r\right)\right\}\right]\end{aligned} \tag{26}$$

The identity, $\mathcal{R}\left(k_{\mathrm{E}}^{*}\right)=\mathcal{R}\left(k_{\mathrm{E}}\right)^{*}, \mathbb{H}_0\left(z^{*}\right)=\mathbb{H}_0\left(z\right)^{*}$, and $Y_0\left(z^{*}\right)=Y_0\left(z\right)^{*}$ were used. The displacement function 26 shows that the real pole k_{T} corresponds to travelling waves and the two complex poles k_{D}, and k_{E} correspond to damped travelling waves.

4 Surface strain

The surface strain for point loading is

$$s\left(r\right)=-\frac{h}{2}\frac{d^2}{dr^2}\eta\left(r\right) \tag{27}$$

pointing in the radial direction, since the Green's function is a function of distance from the point of forcing, only. Using equation 12 (and Abramowitz and Stegun [4] formulas 9.1.27)

$$s\left(r\right)=-\frac{ih}{4}\sum_{\kappa\in\hat{K}}\mathcal{R}\left(\kappa\right)\left(\kappa^2H_2^{(1)}\left(\kappa r\right)-\frac{\kappa}{r}H_1^{(1)}\left(\kappa r\right)\right) \tag{28}$$

Figure 8 is a plot of function 28.

Note that the real component has the singularity at $r=0$.

4.1 Strain in the near field

The displacement in the near field, r small and possibly 0, is given by equation 17 in which the non-constant terms have the terms with $l\geq 1$ have the r-dependence $\left(\log\left(\kappa r\right)+c\right)\left(\kappa r\right)^{2l}$ for some constant c. The second derivative for each term is

$$\frac{d^2}{dr^2}\left(\log\left(\kappa r\right)+c\right)\left(\kappa r\right)^{2l}=\kappa^{2l}r^{2l-2}\left(\left(2l-1\right)\left(2l\left(\ln\kappa r+c\right)\right)+2l+1\right)$$

which is non-zero at $r=0$ only for the $l=1$ term. That term can be written

$$\frac{-1}{\pi}\sum_{\kappa\in\hat{K}}\mathcal{R}\left(\kappa\right)\left(\frac{\kappa^2r^2}{4}\left(\psi\left(2\right)-\log\kappa-\log r+\log 2-i\frac{\pi}{2}\right)\right).$$

In general the term

$$\sum_{\kappa\in\hat{K}}\mathcal{R}\left(\kappa\right)\kappa^2$$

is real but not zero. Hence, the strain has a singularity at the origin that behaves like $\log r$ plus a constant and is in phase with the forcing.

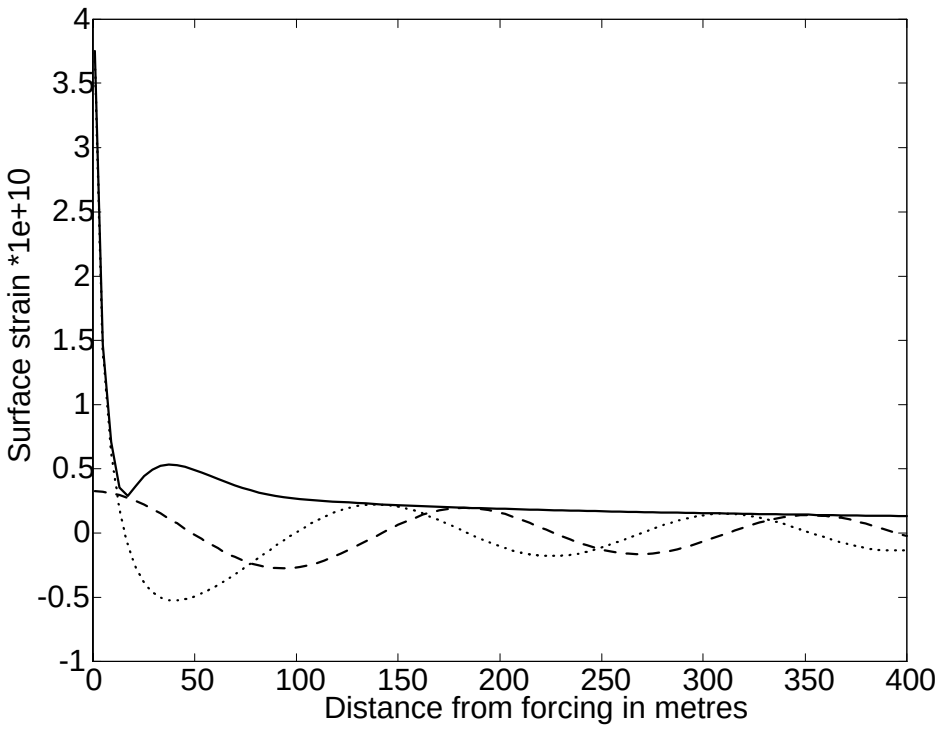

Figure 8: Strain at surface of ice for unit forcing in the running example, Period of 10 seconds, water depth 1000 metres and ice thickness of 1 metre. Real part dashed line, imaginary part dotted line, magnitude solid line.

4.2 Strain in the far field

When r is large the surface displacement given by equation 18. The strain form equation 27 is then

$$\begin{aligned} s(r) &= -\frac{h}{2}\frac{\partial^2 \eta}{\partial r^2} = \frac{h}{2}\frac{\mathcal{R}_{\mathrm{T}}}{\sqrt{2\pi k_T}}\left(\frac{k_T^2}{\sqrt{r}} + i\frac{k_T}{r^{3/2}} - \frac{3}{4}\frac{1}{r^{5/2}}\right)\exp\left\{i\left(k_{\mathrm{T}} r + \pi/4\right)\right\} \\ &\approx \frac{h}{2}\frac{k_{\mathrm{T}}^2 \mathcal{R}_{\mathrm{T}}}{\sqrt{2\pi k_{\mathrm{T}}}}\frac{\exp\left\{i\left(k_{\mathrm{T}} r + \pi/4\right)\right\}}{\sqrt{r}} \end{aligned}$$

for large r. The strain direction is in the radial direction only. Hence the maximum strain is given by the complex magnitude of $s(r)$.

Figure 9 shows the magnitude of strain at $r = 500$ metres for a range of ice thicknesses as a function of period. In all cases the water depth is 1000 metres. Note that the strain for 0.5 metre ice is considerably greater than the other thicknesses shown.

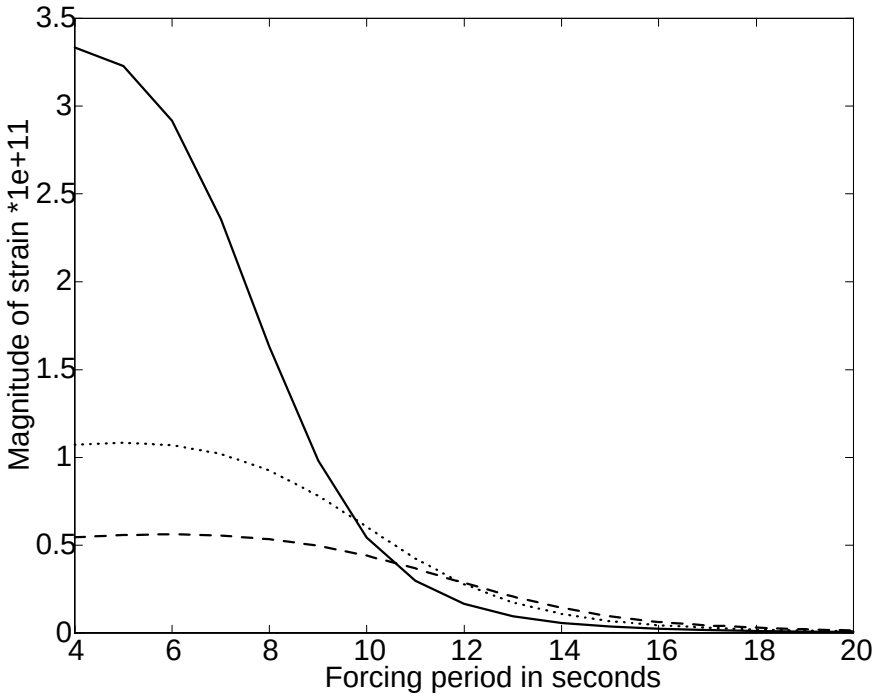

Figure 9: The amplitude of strain function at $r = 500$ metres at a range of forcing periods, 4 seconds to 20 seconds, for various thickness of ice. Solid line: 0.5 metre, dotted line: 1.0 metre, dashed line: 1.5 metre.

5 Some results in graph form

Here are graphs of magnitudes of residues, displacement, strain for the periods T=4,5,7,10,15,20 seconds and $H = 1000$ metres, $h_{\mathrm{i}} = 1$ metre.

5.1 Residues

The following sequence of graphs show the residues, indexed by the order that the corresponding pole appears in $\hat{K}$. The first residue is for the travelling mode, the second and third for the damped travelling modes, and the remainder for evanescent modes. The graphs from (a) to (f) are for the geometry $H = 1000$ metres, $h_{\mathrm{i}} = 1$ metre and for the periods T=4,5,7,10,15,20 seconds respectively. The value E=6×10^9 has been used for the effective Young's modulus.

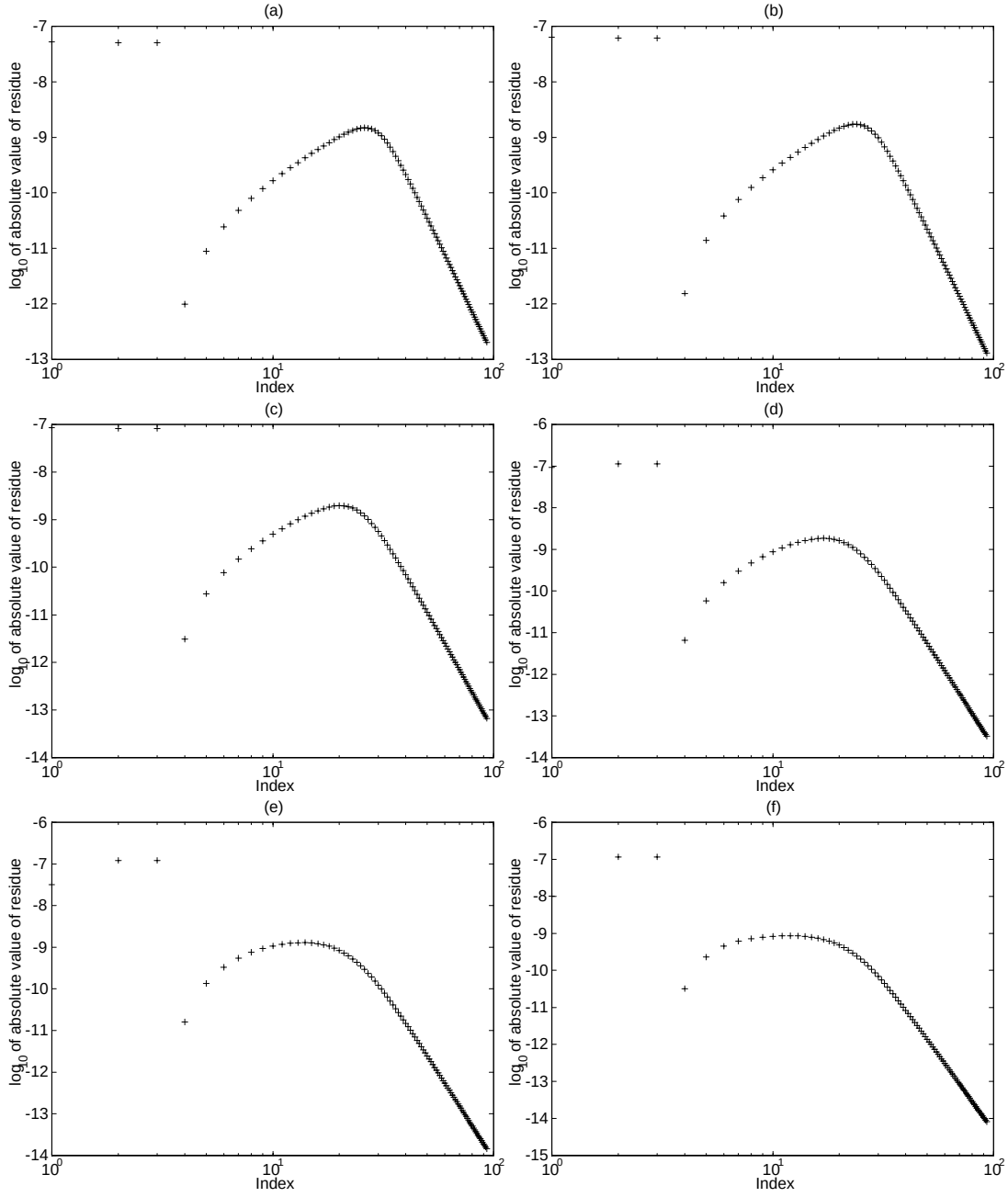

5.2 Surface displacement

The following graphs from (a) to (f) show the surface displacement for the same geometry and range of periods as used in the previous series of graphs of the residues. The real (in-phase) part is shown as a dashed line, the imaginary (quadrature) part is shown as a dotted line, and the magnitude is shown as a solid line.

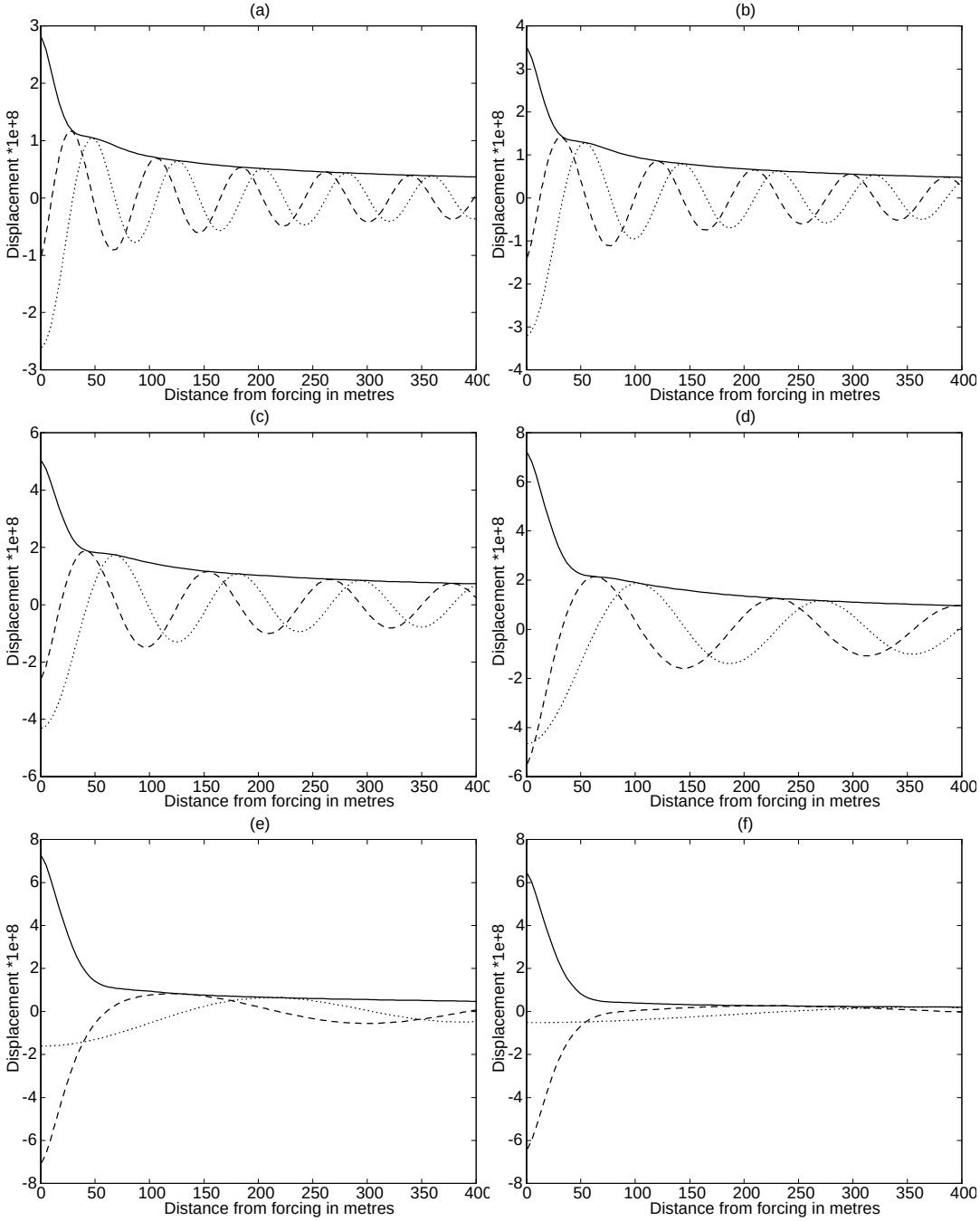

5.3 Surface strain

The following graphs from (a) to (f) show the surface strain for the same geometry and range of periods as used in the series of graphs of residues. The real (in-phase) part is shown as a dashed line, the imaginary (quadrature) part is shown as a dotted line, and the magnitude is shown as a solid line. Note that the real part is singular at $r = 0$.

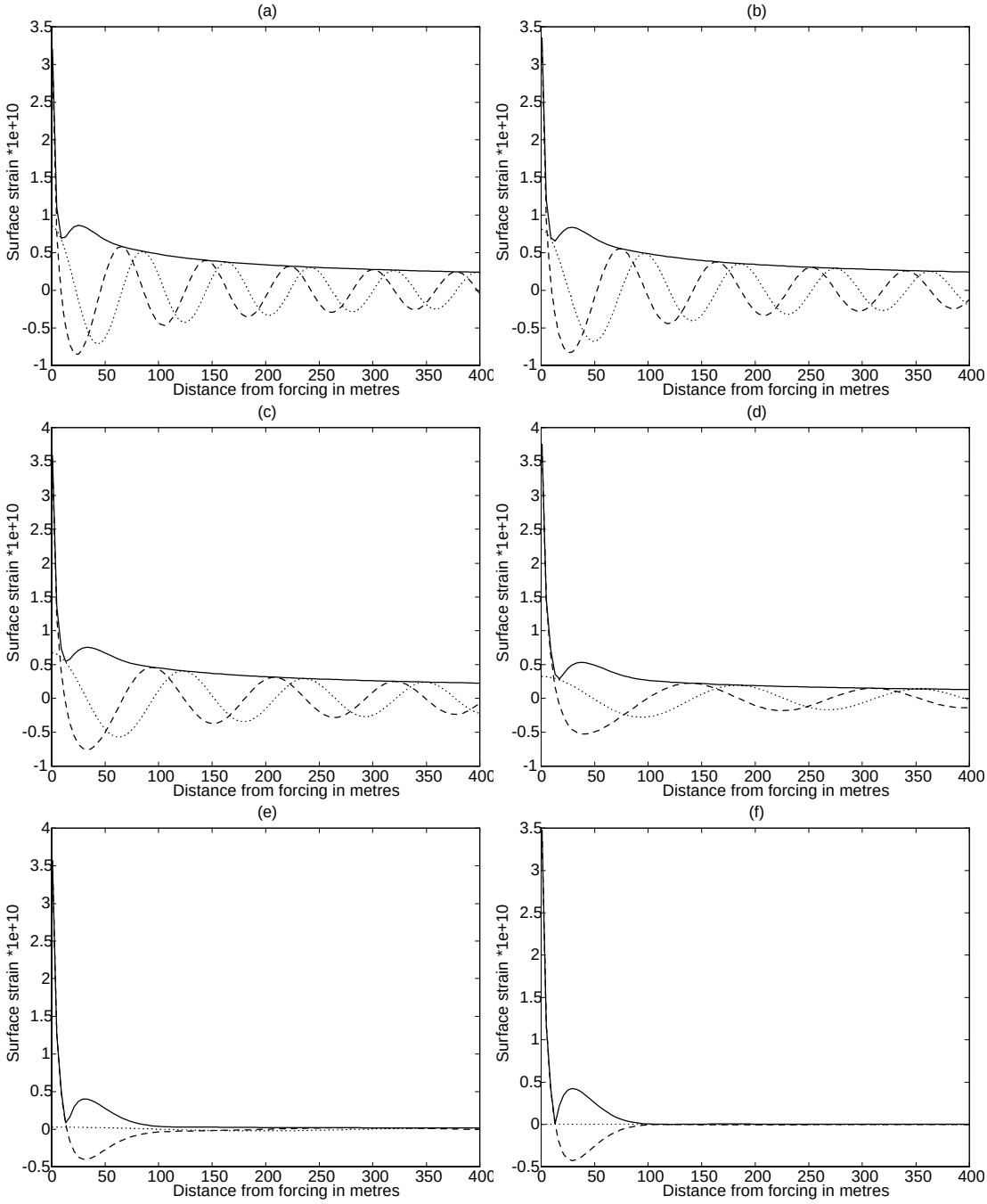

One interesting feature of the strain is the peak in strain magnitude at about 40m from the point of forcing. The following pair of graphs shows magnitude of that peak and the distance from the point of forcing at which that the peak occurs as a function of period of forcing. The geometry $H = 1000$ metres, $h_{\mathrm{i}} = 1$ metre is as in the previous graphs.

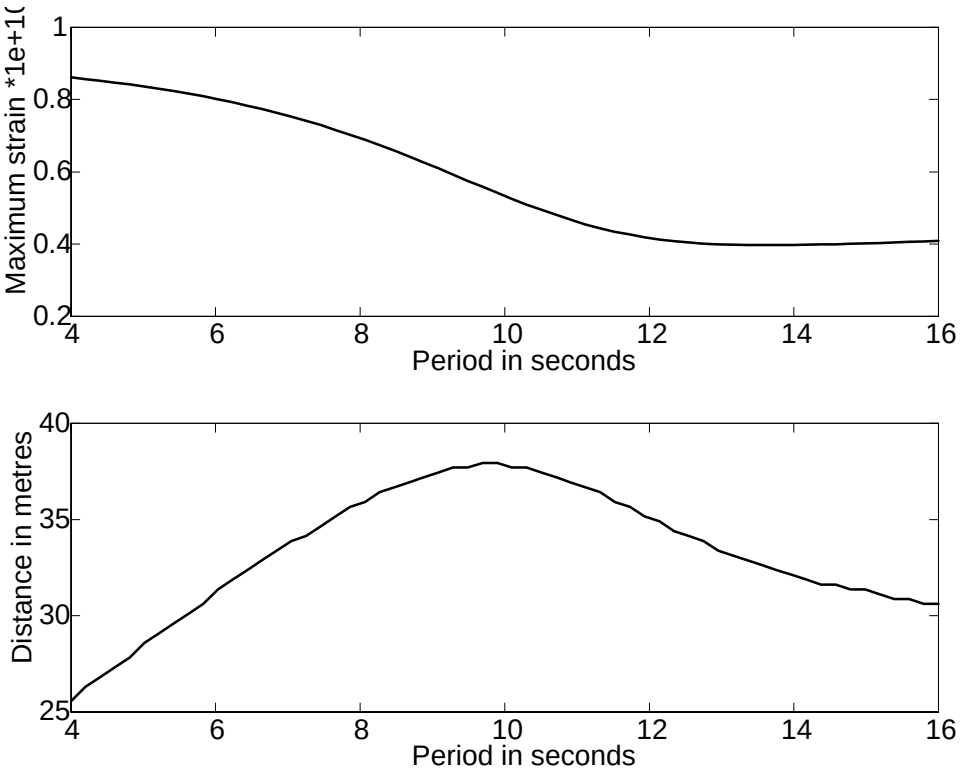

Magnitude of peak (top figure) and position of peak (lower figure) for 1metre thick ice.

Here are the analogous graphs for the same range of parameters except $h_{\mathrm{i}} = 0.5$m.

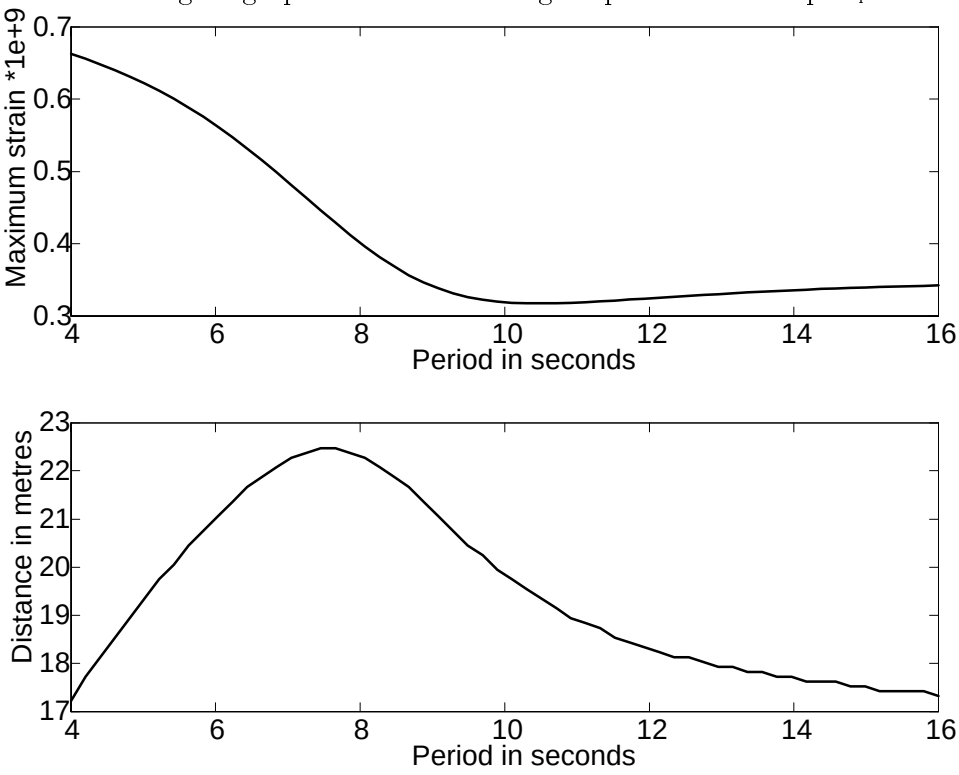

Magnitude of peak (top figure) and position of peak (lower figure) for 0.5 metre thick ice.

Note that the distance to the peak strain scales as the characteristic length while the period at which the peak occurs scales as the square-root of the characteristic lengths.

References

[1] Fox, C., & Squire, V.A. 1994 On the Oblique Reflexion and Transmission of Ocean Waves at Shore Fast Sea Ice. *Phil. Trans. R. Soc. Lond.* A (1994) **347**, 185-218.

[2] Bracewell, Ron 1965 *The Fourier Transform and its Applications*. McGraw-Hill.

[3] Smirnov, V. I. 1964 *A Course of Higher Mathematics* Volume III part 2. Pergamon Press.

[4] Abramowitz, M. & Stegun, I.A. 1972 *A Handbook of Mathematical Functions*. Dover Publications, New York .

[5] Wymann, Max. 1950 Deflections of an Infinite Plate, *Canadian Journal of Research*, **28**, sec. A.

[6] Fox, C., Wilcocks, L. & Haskell, T. 1996 A Calculation of Sea-Ice Young's Modulus Using Under-Ice Pressure Measurements. Dept. Math. Report 335, The University of Auckland, ISSN 1173-0889.

[7] Bateman, H. 1954 *Tables of Integral Transforms* Volume II. McGraw-Hill.

A Special functions

Power series expansions for the modified Bessel functions I_0 and K_0 are given in Abramowitz and Stegun [4] in formulas 9.6.12 and 9.6.13, respectively, and are

$$\begin{aligned} I_0(z) &= \sum_{k=0}^{\infty} \frac{(z/2)^{2k}}{(k!)^2}, \\ K_0(z) &= -\log\left(\frac{z}{2}\right) I_0(z) + \sum_{k=0}^{\infty} \frac{(z/2)^{2k}}{(k!)^2} \psi(k+1) \end{aligned}$$

where ψ is the Psi function for positive integer argument defined by ([4] formula 6.3.2)

$$\begin{aligned} \psi(1) &= -\gamma, \\ \psi(k+1) &= \left(\sum_{n=1}^{k} \frac{1}{n}\right) - \gamma, \quad k \geq 1 \end{aligned}$$

in which $\gamma = 0.5772156649015325\cdots$ is Euler's constant.

Since $I_0(0) = 1$ and $\psi(1) = -\gamma$, the modified Bessel function the second kind, $K_0(z)$, tends to $-\log(z) - \gamma + \log 2$ near the origin and is singular at $z = 0$.

B Series expansion of $\eta(k)$

We wish to expand $\eta(k)$ as a sum of terms like $R/(k-a)$ over poles a of η. We first establish general conditions for such an expansion to exist, and then show that those conditions are satisfied by η as given in equation 5.

B.1 Series expansion of fractional functions

We consider a function that is regular in the whole plane except at isolated points. Such a function is known as fractional function. We show that a fractional function that has an infinite number of poles can be expressed by infinite series of polynomials[3].

Let $f(z)$ be a fractional function that has an infinite number of poles. We note that a number of poles that are situated within a bounded region is always finite since the set of poles does not have limit-points. Indeed, if there is a limit-point $z = c$ then any small circle with centre at $z = c$ would contain an infinite number of poles. Once we have a finite number of poles in a confined part of the plane we can number them in the order of their non-decreasing moduli, so that denoting the poles by a_k we have

$$|a_1| \leq |a_2| \leq |a_3| \leq ...,$$

where $|a_k| \to \infty$ as $k \to \infty$. At every pole $z = a_k$ the function $f(z)$ will have a definite infinite part, which will be a polynomial with respect to the argument $1/(z - a_k)$ without the constant term. We denote this polynomial term by

$$G_k\left(\frac{1}{z - a_k}\right), \; k = 1, 2, 3, \ldots . \tag{29}$$

We show that the fractional function $f(z)$ can be represented by a simple infinite series of G_k by making certain additional assumptions. Suppose that a sequence of closed contours C_n which surround the origin exists and satisfy following conditions:

C1 Non of poles of $f(z)$ are on the contours C_n, $n = 1, 2, 3, ...$

C2 Every contour C_n lies inside the contour C_{n+1}.

C3 Let l_n be length of the contour C_n and δ_n be its shortest distance from the origin then $\delta_n \to \infty$ as $n \to \infty$, i.e., the contours C_n widen indefinitely in all directions as n increases.

C4 A positive number m exists such that

$$\frac{l_n}{\delta_n} \leq m \text{ for any } n.$$

We now suppose that given such a sequence of contours, there exists a positive number M, such that on any contour C_n our fractional function $f(z)$ satisfies

$$|f(z)| \leq M \tag{30}$$

Consider the integral

$$\frac{1}{2\pi i}\int_{C_n}\frac{f(z')}{z'-z}dz' \tag{31}$$

where the point z lies inside C_n and is other than a_k (the poles inside C_n.) We also consider the sum of the polynomials 29 for the poles a_k, inside C_n,

$$\omega_n(z) = \sum_{(C_n)} G_k\left(\frac{1}{z-a_k}\right). \tag{32}$$

The integrand of 31 has a pole $z' = z$ and poles $z' = a_k$. We can calculate the residue at the pole $z' = z$ by

$$\left.\frac{f(z')}{(z'-z)'}\right|_{z'=z} = f(z')\big|_{z'=z} = f(z).$$

The residues at the poles $z' = a_k$ are, by the definition 32, the same as the residues of the function

$$\frac{\omega_n(z')}{z'-z}. \tag{33}$$

We note that all poles of this function are situated inside C_n. We now show that the sum of residues of the function 33 at the poles a_k is

$$-\omega_n(z) = -\sum_{(C_n)} G_k\left(\frac{1}{z-a_k}\right). \tag{34}$$

Since the definition of ω_n and G_k is a polynomial of $1/(z-a_k)$, the order of the denominator of function 33 is at least two units higher than that of the numerator of function 33. Hence, for a circle with a sufficiently large radius R we have

$$2\pi i\sum_{(C_n)}\operatorname*{Res}_{z'=a_k}\frac{\omega_n(z')}{z'-z} = \oint_{C_R}\frac{\omega_n(z')}{z'-z}dz'.$$

The LHS of this does not change as the radius R increases, and the RHS$\rightarrow 0$ as $R \rightarrow \infty$. Indeed,

$$\left| \oint_{C_R} \frac{\omega_n(z')}{z'-z} dz' \right| \leq \oint_{C_R} \left| z' \frac{\omega_n(z')}{z'-z} \frac{1}{z'} dz' \right| \leq \max_{|z'|=R} \left| z' \frac{\omega_n(z')}{z'-z} \right| \frac{2\pi R}{R}$$

and the term $|\cdot|$ tends to zero as $R \rightarrow \infty$. Thus, the sum of residues at poles within a finite distance is zero. Since we know that the residue of 33 at $z' = z$ is $\omega_n(z)$, the sum of the rest is 34. Thus, we have an expression for the integral 31,

$$\frac{1}{2\pi i} \int_{C_n} \frac{f(z')}{z'-z} dz' = f(z) - \sum_{(C_n)} G_k \left(\frac{1}{z-a_k} \right). \tag{35}$$

Also, when $z = 0$ we have

$$\frac{1}{2\pi i} \int_{C_n} \frac{f(z')}{z'} dz' = f(0) - \sum_{(C_n)} G_k \left(-\frac{1}{a_k} \right). \tag{36}$$

Subtracting equation 35 from equation 36 gives

$$\frac{z}{2\pi i} \int_{C_n} \frac{f(z')}{z'(z'-z)} dz' = f(z) - f(0) - \sum_{(C_n)} \left[G_k \left(\frac{1}{z-a_k} \right) - G_k \left(-\frac{1}{a_k} \right) \right].$$

We prove that LHS of t\hi expression tends to zero as $n \rightarrow \infty$.

Since $|z'| \geq \delta_n,\ |z'-z| \geq |z'| - |z| \geq \delta_n - |z|$, we have

$$\begin{aligned} \left| \int_{C_n} \frac{f(z')}{z'(z'-z)} dz' \right| &\leq \frac{M l_n}{\delta_n (\delta_n - |z|)} \\ &< \frac{Mm}{\delta_n - |z|}. \end{aligned} \tag{37}$$

Since $\delta_n \rightarrow \infty$ as $n \rightarrow \infty$, integral in 37 tends to zero as n increases. Note that we used the condition in equation 30 and condition (C4).

Finally, we have formula for $f(z)$,

$$f(z) = f(0) + \lim_{n \rightarrow \infty} \sum_{(C_n)} \left[G_k \left(\frac{1}{z-a_k} \right) - G_k \left(-\frac{1}{a_k} \right) \right].$$

Since, the contour C_n will widen indefinitely as n increases,the second term is a sum over all poles, so we have $f(z)$ in the form of an infinite series

$$f(z) = f(0) + \sum_{k=1}^{\infty} \left[G_k \left(\frac{1}{z-a_k} \right) - G_k \left(-\frac{1}{a_k} \right) \right]. \tag{38}$$

B.2 Conditions for $\eta(k)$

We define a sequence of square contours

$C_n =$ square with its four corners at $\delta_n - i\delta_n, \delta_n + i\delta_n, -\delta_n + i\delta_n,$ and $-\delta_n - i\delta_n,$

where $\delta_n = \left(n + \frac{1}{2}\right)\pi/H$, $n = N, N+1, ...$ The function which we would like to estimate on the contours C_n is

$$\eta(k) = \frac{-1}{Lk^4 - m\omega^2 + g\rho - \dfrac{\rho\omega^2}{k\tanh(kH)}}.$$

We show that $|\eta(k)|$ is bounded on any C_n in order to apply the method introduced above. The function η has two real poles, four complex poles, and an infinite number of imaginary poles.

For the sake of simplicity we write the function $\eta(k)$ as

$$\eta(k) = \frac{-1}{Lk^4 + A - \frac{B}{k\tanh(kH)}}.$$

When $\operatorname{Im} k$ is large the poles of η are almost $\pm in\pi/H$. In fact, the poles ik_n ($k_n \in \mathbb{R}$) of $\eta(k)$ satisfy

$$\frac{1}{(Lk_n^4 + A)\,k_n} = \tan(k_n H),$$

so $k_n \to \pm n\pi/H$ as k_n increases. Thus, by choosing N large the contours C_n are certain distance away from the poles for any $n \geq N$. We prove the boundedness of $|\eta|$ by showing that $|\eta(x+iy)|$ is bounded for $y = \pm\delta_n$, $n = N, N+1, ...$, $x \in \mathbb{R}$ and then for $x = \pm\delta_n$, $n = N, N+1, ...$, $y \in [-\delta_n, \delta_n]$.

For any $n > N$ we have

$$\begin{aligned} \left|Lk^4 + A\right| &> L|k|^4 + C \\ &= L|x+iy|^4 + C \\ &\geq L\delta_n^4 + C \text{ for any } x \in \mathbb{R},\ y = \delta_n, \end{aligned} \tag{39}$$

where C is a constant determined by A and L. When $y = \delta_n$ we have

$$\begin{aligned} \left|\frac{1}{k\tanh(kH)}\right| &= \left|\frac{e^{2xH}e^{i2yH} + 1}{(x+iy)\left(e^{2xH}e^{i2yH} - 1\right)}\right| \\ &= \frac{\left|e^{2xH}e^{i2yH} + 1\right|}{|x+iy|\left|e^{2xH}e^{i2yH} - 1\right|} \\ &= \frac{\left|e^{2xH} - 1\right|}{|x+iy|\left|e^{2xH} + 1\right|} \leq \frac{1}{|x+iy|} \leq \frac{1}{\delta_n} \end{aligned} \tag{40}$$

for any $x \in \mathbb{R}$. We used $\exp(i(2n+1)\pi) = -1$ and

$$\left|\frac{e^{2xH} - 1}{e^{2xH} + 1}\right| \leq 1.$$

For large N we have

$$\left|Lk^4 + A - \frac{B}{k\tanh(kH)}\right| \geq \left|Lk^4 + A\right| - \left|\frac{B}{k\tanh(kH)}\right|.$$

Since RHS of this inequality is positive from 39 and 40,

$$\begin{aligned} |\eta(k)| &\leq \frac{1}{|Lk^4 + A| - \left|\frac{B}{k\tanh(kH)}\right|} \\ &\leq \frac{1}{L\delta_n^4 + C - \frac{B}{\delta_n}} \\ &\leq \frac{1}{L\delta_N^4 + C - \frac{B}{\delta_N}} \text{ for any } n \geq N. \end{aligned} \tag{41}$$

Note that the same relationship holds for $y = -\delta_n$.

For k on the line segment $\delta_n - i\delta_n$ to $\delta_n + i\delta_n$ we use the fact that

$$\begin{aligned} & \frac{\left|e^{2xH}e^{i2yH} + 1\right|}{|x+iy|\,|e^{2xH}e^{i2yH} - 1|} \\ \leq\ & \frac{1}{|x+iy|}\frac{1 + \left|e^{-2xH}\right|}{1 - |e^{-2xH}|} \\ \leq\ & \frac{D_N}{\delta_N} \text{ for any } y,\ n \geq N \end{aligned}$$

since,

$$\frac{1 + \left|e^{-2xH}\right|}{1 - |e^{-2xH}|} \leq \frac{1 + \left|e^{-2\delta_N H}\right|}{1 - |e^{-2\delta_N H}|} = D_N\ ,\ \frac{1}{|x+iy|} \leq \frac{1}{\delta_N}.$$

From equation 39 and the first line of equation 41, we have

$$\frac{1}{|Lk^4 + A| - \left|\frac{B}{k\tanh(kH)}\right|} \leq \frac{1}{L\delta_N^4 + C - \frac{BD_N}{\delta_N}} \text{ for any } n \geq N.$$

The same proof can be applied for the line segment $-\delta_n - i\delta_n$ to $-\delta_n + i\delta_n$. We have proved that $|\eta(z)|$ is bounded on all contours C_n, $n \geq N$ where N is chosen to be large so that the contours are certain distance away from all the poles of η.

B.3 Expansion of $\eta(k)$

As we have seen in the previous section, the function $\eta(k)$ satisfies all the conditions C1∼C4, and if we omit the imaginary part of the denominator of η created by the damping coefficient β, we notice that the function η has a countably-infinite number of imaginary poles, two real poles, and four complex poles[1]. Hence, we can expand the function $\eta(k)$ as a sum over infinite fractional polynomials. Let $R(\kappa)$ be the residue at $k = \kappa$, then the polynomial term 29 is

$$G_\kappa\left(\frac{1}{k-\kappa}\right) = \frac{R(\kappa)}{k-\kappa}.$$

Hence, the expansion of $\eta(k)$ becomes, from the formula 38 and $\eta(0) = 0$,

$$\begin{aligned} \eta(k) &= \sum_\kappa \left[\frac{R(\kappa)}{k-\kappa} + \frac{R(\kappa)}{\kappa}\right] \\ &= \sum_{\kappa \in \hat{K}} \left[\frac{2\kappa R(\kappa)}{k^2 - \kappa^2} + \frac{2R(\kappa)}{\kappa}\right]. \end{aligned}$$

Note that the summation on the first line is over all poles of $\eta(k)$. We used that $R(\kappa) = R(-\kappa)$, since $\eta(k)$ is an even function and

$$-(k-\kappa)\eta(k) = (-k+\kappa)\eta(-k) = (k+\kappa)\eta(k)$$

so,

$$-\lim_{k\to\kappa}(k-\kappa)\eta(k) = \lim_{k\to-\kappa}(k+\kappa)\eta(k).$$

At the first glance, this formula seems different from the formula **??**. However, the term $\sum 2R(\kappa)/\kappa$ is zero. Indeed, expansion of the function $\eta(k)k$ which satisfies the conditions C1∼C4 and has the same poles as the function $\eta(k)$ and residues $R(\kappa)\kappa$ at $k = \kappa$. Hence, $\eta(k)k$ expanded as,

$$\begin{aligned}\eta(k)k &= \sum_{\kappa}\left[\frac{\mathcal{R}(\kappa)}{k-\kappa} + \frac{\mathcal{R}(\kappa)}{\kappa}\right] \\ &= \sum_{\kappa\in\hat{K}}\frac{2k\mathcal{R}(\kappa)}{k^2-\kappa^2}.\end{aligned}$$

where $\mathcal{R}(\kappa) = \kappa R(\kappa)$. We used that $\mathcal{R}(\kappa) = \mathcal{R}(-\kappa)$.

The fact that $\sum 2R(\kappa)/\kappa$ is zero can also be confirmed by using the contour integration of the function $\eta(k)/k$ as in the figure 4.

The function $\eta(k)/k$ is an odd function and has the same poles as the function $\eta(k)$ with the residues $R(\kappa)/\kappa$. Notice that $k = 0$ is not a singular point of $\eta(k)/k$. Hence, the integration over the real axis is zero and $\eta(k)/k \to 0$ on the semi-arc with order of R^{-3} as $R \to \infty$. Hence, we have

$$\sum_{\kappa\in\hat{K}}\frac{2R(\kappa)}{\kappa} = 0.$$

C MatLab code

C.1 Root finding code

The following code finds the roots of the dispersion equation with $\beta = 0$, and calculates the corresponding residues of $\eta(k)$.

```
function [kice,residR]=rootnresid(t,hwater,hice,nevsc)
% ROOTSNRESID Complex roots of the dispersion equations and associated
% residues.
% Call as [Kice,Resid]=rootnresid(T,Hwater,Hice,nevsc)
% Kice are the k-numbers for the waves in the ice-covered sea.
% Resid are the associated residues

% Author: Colin Fox
% Modified from COROOTS 2 September 1998

[p,g,w,L,a,b,dwater,dice] = setparam(t,hwater,hice);
% Find the ice-covered-sea travelling root
% Use an approximation as a starting guess (ref 17 Jan 1990)
k1=(b/L)^.2;
```

```
% Use the asymptote as a lower bound on the root
if a < 0, kmin=(-a/L)^.25; k1=kmin+abs(k1-kmin); else kmin=0; end
% Now bracket the root
if ftice(k1,p) >= 0,
  k2= (kmin+k1)/2;
  while ftice(k2,p) >= 0, k1=k2; k2=(kmin+k1)/2; end
else
  k2=2*k1;
  while ftice(k2,p) < 0, k1=k2; k2=2*k1; end
end
% and call root finder
ktice=fpzero('ftice',[k1;k2],p);

% Find the evanescent roots
keice=zeros(nevsc,1);
dk=pi/hwater;
index=[1:nevsc]; ks=[(index-.5)*dk; index*dk];
for ind=index,
  if (feice(ks(1,ind),p) * feice(ks(2,ind),p)) > 0,
    keice(ind)=fpzero('feice',ks(:,ind)-.5*dk,p);
  else
    keice(ind)=fpzero('feice',ks(:,ind),p);
  end
end

% Find the damped-travelling-wave k-number using a fixed point algorithm
zr=exp(i*2*pi/5);
kdold=0; kd=(i*b/L)^.2; niter=0; nitermax=100; tiny=1e-15;
while (abs(kd - kdold) >= abs(kd)*tiny) & (niter<=nitermax),
  kdold=kd; niter=niter+1;}
  kd=((-b/tan(kdold*hwater)-a*kdold)/L)^.2;}
  while (real(kd)<0) | (imag(kd)<0), kd=kd*zr; end
end
if niter == nitermax, disp('kd may not be accurate'); end

% Put the roots together
kice = [ktice; conj(-i*kd); i*kd; i*keice];

% Calculate the residual via polynomial (of eta*k)
k2 = kice.^2;
term1 = 5*L*k2;
term2 = a./k2;
term3 = (hwater/b)*((L*kice.^5 + a*kice).^2 - b^2)./k2;
residR = -1./(term1 + term2 + term3);
```

Two functions are called by the root finding code. The first sets up the physical parameters.

```
function [p,g,w,L,a,b,dwater,dice] = setparam(period,hwater,hice)
% SETPARAM makes the vector parameter p which is passed to the
```

```
% dispersion equations via the root finders. Call as
% [p,g,w,L,a,b,dwater,dice] = setparam(period,Hwater,Hice)

% Some physical constants
dwater=1025; dice=922.5; nu=0.3; g=9.8; e=6*10^9;

% Generate a few constants
w = 2*pi/period;
L = e*hice^3/(12*(1-nu^2));
a = dwater*g - dice*hice*w^2;
b = dwater*w^2;

% Store these in a single vector as a parameter for dispersion equation
% functions
p = [ g hwater w L a b ];
```

The second is a variant of MatLab's zero-finding code, modified to accept a parameter for the function and also to take an initial bracket of the root.

```
function b = fpzero(FunFcn,x,param,tol,trace)
%FPZERO Zero of a function of one variable and a constant parameter.
% FPZERO(F,X,PARAM) finds a zero of f(x,param). F is a string containing
% the name of a real-valued function of a single real variable and
% constant parameter. If X is a scalar on entering FPZERO then it is used
% as a starting guess. Optionally X can be a 2-element column vector
% in which case the two values are used to initially bracket the root.
% If they do not bracket a root, i.e., if F(X(1)) and F(X(2)) have the
% same sign the interval will be extended until a root is bracketted.
% PARAM is the, possibly vector, parameter to be passed to F.
% The value returned is near a point where F changes sign.
%
% An optional fourth argument sets the relative tolerance for the
% convergence test. The presence of an nonzero optional fifth
% argument triggers a printing trace of the steps.

% fpzero made from Matlab's fzero by Colin Fox, 16 January 1990.
% Modified by CF 17-Jan-90 to accept initial bracketting of the root

% Initialization
if nargin < 4, trace = 0; tol = eps; end
if nargin == 4, trace = 0; end
if trace, clc, end
% Deal with scalar or vector starting guess
temp=size(x);
if temp(1) >= 2,
  a = x(1); fa = feval(FunFcn,a,param);
  if trace, home, init = [a fa], end
  b = x(2); fb = feval(FunFcn,b,param);
  if trace, home, init = [b fb], end
  x = (a+b)/2; dx = (b-a)/2;
```

```
else
% For scalar x perform the original matlab initial interval making procedure
  if x ~= 0, dx = x/20;
  else, dx = 1/20;
  end
  a = x - dx; fa = feval(FunFcn,a,param);
  if trace, home, init = [a fa], end
  b = x + dx; fb = feval(FunFcn,b,param);
  if trace, home, init = [b fb], end
end
% Find, or ensure, a change of sign.
while (fa > 0) == (fb > 0)
  dx = 2*dx;
  a = x - dx;
%[m,n]=size(a); if (n~=1 | m~=1), keyboard, end
  fa = feval(FunFcn,a,param);
  if trace, home, sign = [a fa], end
  if (fa > 0) ~= (fb > 0), break, end
  b = x + dx; fb = feval(FunFcn,b,param);
  if trace, home, sign = [b fb], end
end
fc = fb;
% Main loop, exit from middle of the loop
while fb ~= 0
  % Insure that b is the best result so far, a is the previous
  % value of b, and c is on the opposite of the zero from b.
  if (fb > 0) == (fc > 0)
    c = a; fc = fa;
    d = b - a; e = d;
  end
  if abs(fc) < abs(fb)
    a = b; b = c; c = a;
    fa = fb; fb = fc; fc = fa;
  end
  % Convergence test and possible exit
  m = 0.5*(c - b);
  toler = 2.0*tol*max(abs(b),1.0);
  if (abs(m) <= toler) + (fb == 0.0), break, end
  % Choose bisection or interpolation
  if (abs(e) < toler) + (abs(fa) <= abs(fb))
    % Bisection
    d = m; e = m;
  else
    % Interpolation
    s = fb/fa;
    if (a == c)
      % Linear interpolation
      p = 2.0*m*s;
```

```
      q = 1.0 - s;
    else
      % Inverse quadratic interpolation
      q = fa/fc;
      r = fb/fc;
      p = s*(2.0*m*q*(q - r) - (b - a)*(r - 1.0));
      q = (q - 1.0)*(r - 1.0)*(s - 1.0);
    end;
    if p > 0, q = -q; else p = -p; end;
    % Is interpolated point acceptable
    if (2.0*p < 3.0*m*q - abs(toler*q)) * (p < abs(0.5*e*q))
      e = d; d = p/q;
    else
      d = m; e = m;
    end;
  end % Interpolation
  % Next point
  a = b;
  fa = fb;
  if abs(d) > toler, b = b + d;
  else if b > c, b = b - toler;
    else b = b + toler;
    end
  end
  fb = feval(FunFcn,b,param);
  if trace, home, step = [b fb], end
end % Main loop
```

The root finder uses different forms of the dispersion equation depending on whether the root is pure imaginary or pure real. The first is for the travelling root.

```
function f=ftice(s,p)
% FTWAT is the dispersion equation for the ice-covered-sea in a
% form convenient for finding the travelling wave k-number
% p is the vector parameter

f=tanh(s*p(2)) - p(6)/(p(4)*s^5 + p(5)*s);
```

The second is for the evanescent roots.

```
function f=feice(s,p)
% FEICE is the dispersion equation for the ice-covered-sea in a
% form convenient for finding the evanescent wave k-numbers
% p is the vector parameter

f=(p(4)*s^5+p(5)*s)*sin(s*p(2)) + p(6)*cos(s*p(2));
```

C.2 Code for displacement and strain

The following script file calculates the displacement and strain for a given period, ice thickness, and water depth. The displacement is plotted.

```
% Plot the greens function
T=10;           % period
hice=1;         % ice thickness
hwater=1000;    % water depth
nevsc=100;      % number of evanescent modes to sum over

[kice,residR]=rootsnresid(T,hwater,hice,nevsc);
r=linspace(1,400,100);

% Calculate surface displacement
dice=i*besselh(0,kice(1)*r)*residR(1)/2;
for ind=2:nevsc+3
 dice=dice+i*besselh(0,kice(ind)*r)*residR(ind)/2;
end

plot(r,real(dice),'black--',r,imag(dice),'black:',r,abs(dice),'black-')
title(['T=',int2str(T),'hice=',int2str(hice),'hwater=',int2str(hwater)])
xlabel('Distance from forcing in metres')
ylabel('Displacement')

% Calculate the strain
strain=(i/2)*residR(1)*(besselh(2,kice(1)*r)*kice(1)^2 - ...
                        kice(1)*besselh(1,kice(1)*r)./r);
for ind=2:nevsc+3
 k = kice(ind);
 strain = strain + (i/2)*residR(ind)*(besselh(2,k*r)*k^2 - ...
                                      k*besselh(1,k*r)./r);
end
```